國立政治大學理學院應用物理研究所

碩士論文

Graduate Institute of Applied Physics, College of Science

National Chengchi University

Master Thesis

鉍-銻-碲奈米線之合成、量測與熱電性質

Synthesis, measurements and thermoelectric properties of

$Bi_xSb_{2-x}Te_{3-y}$ nanowires

董光平

Guang-Ping Dong

指導教授: 陳洋元 博士

Advisor: Dr. Yang-Yuan Chen

中華民國一○一年六月

June, 2012

摘要

　　諸多的研究顯示，和塊材相比，低維度的材料其物理性質會有所不同，為了探究熱電材料在低維度下對其熱電性質所造成的效應，我們合成了 $Bi_xSb_{2-x}Te_{3-y}$ 奈米線並量測其熱電性質。本實驗藉由熱處理薄膜製備奈米線的方法合成單晶 $Bi_xSb_{2-x}Te_{3-y}$ 奈米線。我們先利用脈衝雷射沉積系統將 $Bi_xSb_{2-x}Te_3$ 鍍在矽基板上形成薄膜，再將薄膜以 350 ℃ 至 490 ℃ 熱處理 5 到 21 天，奈米線即為了平衡因薄膜與矽基板彼此熱膨脹係數不同所造成的應力而自薄膜上長出，其直徑為幾十奈米至幾百奈米不等，長度則為幾微米至幾十微米。為了瞭解奈米線之構成與量測其熱電性質，我們結合微影製程及操縱技術，將單根奈米線架空於附有電極、加熱元件及溫度感測元件之量測平台上，由於奈米線已被架空，我們便能透過選區繞射分析奈米線其結晶性，並使用能量散射分析儀得知奈米線之成分，利用四點量測可得知奈米線的電阻率 ρ，以加熱元件在奈米線兩端產生溫差，並量測因西貝克效應 (Seebeck effect) 所造成之電壓差即能得到西貝克係數 S (Seebeck coefficient)，三倍頻技術要求所量測的樣品必須要架空於基板上，運用三倍頻技術 (3ω method) 可量測奈米線之熱導率 κ 及比熱。結合微影製程、操縱技術以及量測系統，我們成功得到單根奈米線的三個熱電係數 ρ、S 以及 κ，並了解低維度對熱電性質所造成的影響。

Abstract

Compare with the bulk materials, many researches had revealed that physical properties were different in low dimensional materials. To study the low-dimensional effects on thermoelectric properties of thermoelectric materials, $Bi_xSb_{2-x}Te_{3-y}$ nanowires were synthesized and studied for their thermoelectric properties. Single-crystallized $Bi_xSb_{2-x}Te_{3-y}$ nanowires were synthesized by on-film formation of nanowires. First, $Bi_xSb_{2-x}Te_3$ thin films were deposited on SiO_2/Si substrates by using the pulsed laser deposition system. $Bi_xSb_{2-x}Te_{3-y}$ nanowires grew from the films by annealing the films at 350~490 ℃ for 5~21 days through the stress release of the thermal expansion mismatch between the film and the substrate. A series of $Bi_xSb_{2-x}Te_{3-y}$ nanowires were prepared with the diameter from few tens of nanometers to few hundreds of nanometers and the length from few micrometers to few tens of micrometers. In order to analyze the components and measure the thermoelectric properties of the nanowires, the technique of combining microfabrication and manipulation for suspending a single $Bi_xSb_{2-x}Te_{3-y}$ nanowire on a measurement platform with electrodes, heater and thermometers was developed. As long as the wire is suspended, the crystallization of the nanowire is able to be analyzed by the selected area electron diffraction (SAED). The composition of the nanowire can be analyzed by the STEM-EDX. Resistivity ρ is measured by the four-point probe method. In order to get the Seebeck coefficient S, temperature difference were generated by the heater and thermoelectric voltage generated by Seebeck effect were measured. The 3ω method which demands that the wire should be suspended was applied to measure the thermal conductivity κ and specific heat c. By using the developed technique and the measurement system, three thermoelectric parameter ρ, S, κ of a single nanowire were successfully measured and the low-dimensional effect on thermoelectric properties were examined.

致謝

　　首先我想要感謝的是我的家人們，感謝我很愛很愛的媽媽和爸爸養育我，支持我走到這一步，感謝我很愛很愛的妹妹和弟弟，我們相親相愛，互相扶持，做哥哥的我真的很開心有你們這兩個小的，感謝我很愛很愛的阿公，謝謝你來參加我的畢業典禮，看你穿上我的碩士袍後露出的笑容，讓我覺得一切的努力都是值得的，第一次離開高雄到台北就學，心情既緊張又期待，感謝姑姑、姑丈還有表兄弟姊妹們，讓我在外地求學時有個依靠。

　　感謝陳洋元教授既嚴謹又開放的指導，讓我在實驗上有所發揮並且往正確的方向進行，感謝尚謙學長從我一進實驗室就開始帶著我做實驗直到他畢業，讓我能獨立完成奈米線的製作，還有熊德智學長在我實驗初期帶了我一陣子，讓我對奈米線的量測有初步的了解，非常非常感謝秉中學長，總是給我啟發，為我解惑，在他的帶領下我學到了很多，讓我得以交出成果順利畢業，感謝虹蚚學長、翊誠學長、偉嘉學長在無塵室的製程幫我很多忙，正龍學長和天蔚學長總是不吝色地給我們這些學弟妹們一些指教，我想我永遠不會忘記和政憲、育竹、耀文一起煮麵趕論文的那些日子，特別要感謝政憲在塊材的製作與量測上給我的幫助，感謝慈蓮學姊、佳華學長、Dedi、瀞謙、泓舜、暉閎、琬婷、怡臻、凡芸、寬仁學長和學弟妹們，因為有你們，奈米材料與低溫物理實驗室內總是充滿了歡笑聲，為我的碩士生涯增添好多好多的樂趣，還要特別感謝中央研究院奈米核心設施中心曾傳銘博士在 TEM 分析上的大力協助與郭白嘉學長代為操作 FIB，感謝在碩一與我一起熬夜讀書、寫作業的同學們，特別感謝勛哥告訴我研發替代役的資訊，讓我得以在智慧財產局服役。

Table of Contents

List of figures

Chapter 2

Chapter 3

Chapter 4

List of tables

Chapter 3

Chapter 1

Introduction

Thermoelectric materials can be used to convert thermal energy into electrical energy directly and vice versa. The performance of a thermoelectric material can be judge by the dimensionless parameter $ZT=S^2T/\rho\kappa$ where S is the Seebeck coefficient, T is the used temperature, ρ is the resistivity and κ is the thermal conductivity.

Bulk silicon (Si) has a high thermal conductivity (~150 W/m-K at room temperature), giving $ZT\approx0.01$ at 300 K [1]. Recent report has shown that it is possible to achieve $ZT=0.6$ at room temperature in rough Si nanowires of ~50 nm diameter which were synthesized by an aqueous electroless etching (EE) method [2]. To study low-dimensional effects on thermoelectric properties is very interesting.

Many methods have been used to synthesize the bismuth telluride-based nanowire. For example, chemical electrodeposition is applicable to fabricate nanowires in prepatterned aluminum matrix (AAM) template [3]. In this research, single-crystalline $Bi_xSb_{2-x}Te_3$ nanowires were synthesized by the on-film formation of nanowires [4].

Measuring thermoelectric properties on a same nanowire to obtain ZT is challenging. In this research, we develop the technique to know the composition, crystalline orientation and thermoelectric properties on a same $Bi_xSb_{2-x}Te_3$ nanowire.

Chapter 2

Thermoelectric material

Introduction

This chapter gives an introduction of the thermoelectric effects and thermoelectric material. Section 2.1 gives a brief concept about thermoelectric effect. Section 2.2 discusses the figure of merit for thermoelectric materials.

2.1 Thermoelectric effect

The thermoelectric effect refers to phenomena by which either a temperature difference creates an electric potential or an electric potential creates a temperature difference. These phenomena are known more specifically as the Seebeck effect, Peltier effect, and Thomson effect.

Seebeck effect [5]

When two dissimilar conductors, A and B, constitute a circuit, a current will flow as long as the junctions of the two conductors are at different temperature. Conductor A is defined as being positive to conductor B if the electrons flow from A to B at colder junction.
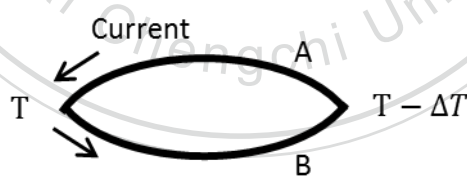
Figure 2.1   The Seebeck effect

If the temperature difference ΔT between the two ends of a material is small, then the Seebeck coefficient which represent as S of a material is conventionally defined as $S = -\Delta V/\Delta T$ where ΔV is the thermoelectric voltage seen at the terminals.

Peltier effect [5]

When an electric current flows across a junction of two dissimilar conductors, heat is liberated or absorbed. When the electric current flows in the same direction as the Seebeck current, heat is absorbed at the hotter junction and liberated at the colder junction. The Peltier effect is defined as the reversible change in heat content when one coulomb crosses the junction.

The direction in which the current flows determines whether heat is liberated or absorbed. This effect is reversible and is independent of the shape or dimension of the materials composing the junction. It is a function of the compositions of the materials and the temperature of the junction, not of the contact.
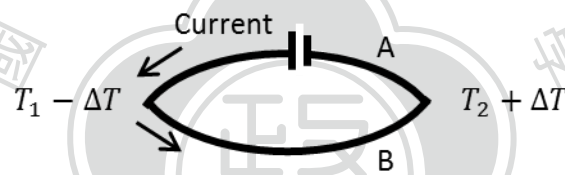
Figure 2.2   The Peltier effect
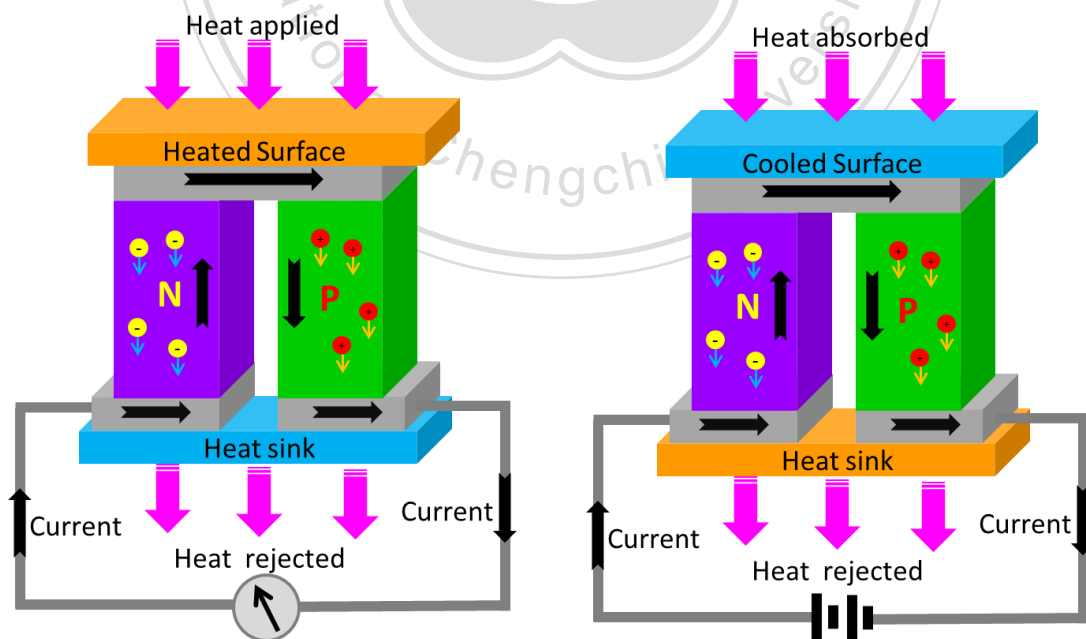
Figure 2.3   (a) The Seebeck circuit configured as a generator. (b) The Seebeck circuit configured as a cooler.

Thomson effect [5]

The Thomson effect is define as the change in the heat content of a single conductor of unit cross section when a unit quantity of electricity flows along it through a temperature gradient of 1K.

Consider a single conductor which has been heated at one point to some temperature T_2. A thermal gradient will exist on either side of the heated point. Two points, P_1 and P_2, of equal temperature, $T_1 < T_2$, will be found on either side of T_2. If current flows in a circuit which include the single conductor, the temperature at P_1 and P_2 will change. These changes are a result of the motion of the electrons with present to the direction of the temperature gradient. The electrons flowing past P_1 will absorb energy in moving against the temperature gradient and increase their potential energy. The electrons following in the same direction as the thermal gradient will give up energy and thus decrease their potential energy.

Heat will accordingly be absorbed at P_1, where the current direction is opposite to the heat flow. Heat will be liberated at P_2, where the current direction is the same as the heat flow. These changes in the heat content of the conductor are the Thomson effect.
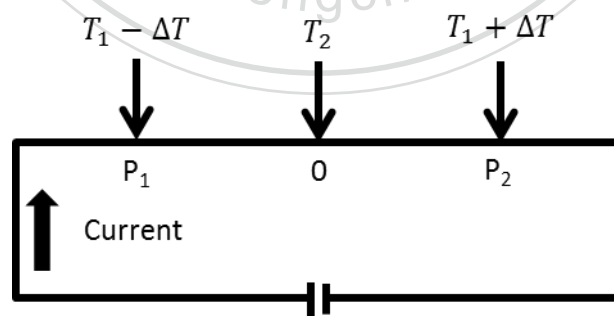
Figure 2.4　The Thomson effect

2.2 Figure of merit

Because thermoelectric materials show the thermoelectric effect in a strong and/or convenient form, it can be demonstrate in power generation and refrigeration.

A figure of merit for the thermoelectric device is defined as $Z=S^2/\rho\kappa$ where S is the Seebeck coefficient, ρ is the resistivity, and κ is the thermal conductivity. The performance of a thermoelectric material can be judged by the dimensionless parameter $ZT=S^2T/\rho\kappa$ where T is the use temperature. A greater ZT indicates a greater thermodynamic efficiency. A good thermoelectric material should have high Seebeck coefficient, low resistivity and low thermal conductivity.
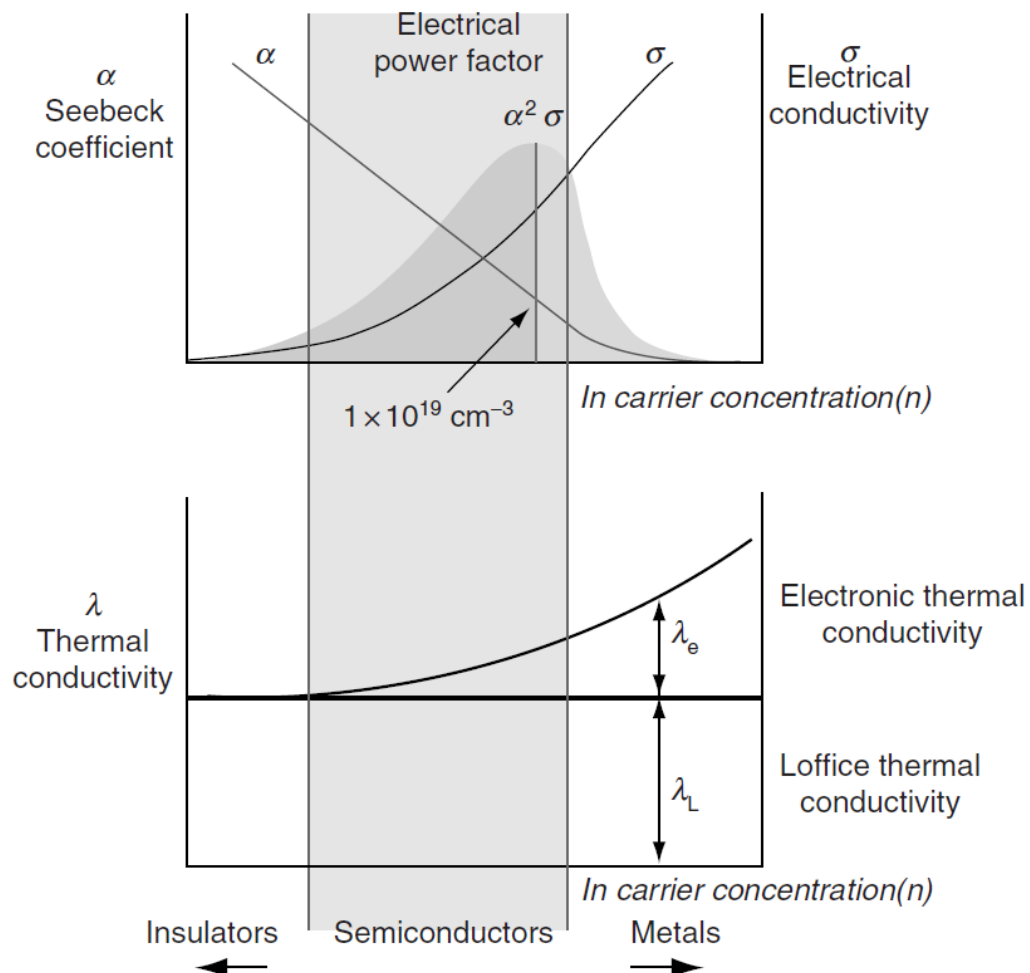
Figure 2.5   Schematic dependence of electrical conductivity, Seebeck coefficient, power factor, and thermal conductivity on concentration of free carriers. [6]

The electrical conductivity is a reflection of the charge carrier concentration and all three parameters which occur in the figure-of-merit are functions of carrier concentration. The electrical conductivity increases with increase in carrier concentration while the Seebeck coefficient decreases, with the electrical power factor maximizing at a carrier concentration of around 10^{25}/cm. The electronic contribution to the thermal conductivity λ_e, which in thermoelectric materials is generally around 1/3 of the total thermal conductivity, also increases with carrier concentration. Evidently the figure-of-merit optimizes at carrier concentrations which corresponds to semiconductor materials.

Chapter 3

Synthesis of nanowires

Introduction

This chapter presents how to synthesize nanowires and the analysis result of the nanowire. Stress-induced method was applied to synthesize nanowires. Section 3.1 introduces the acquired equipment and techniques. Section 3.2 shows how to make the target for the pulsed laser deposition system. Section 3.3 show how to deposit $Bi_xSb_{2-x}Te_3$ thin film by pulsed laser deposition system. Section 3.4 shows the annealing process for growing nanowires. Section 3.5 shows the analysis result of the grown nanowires.
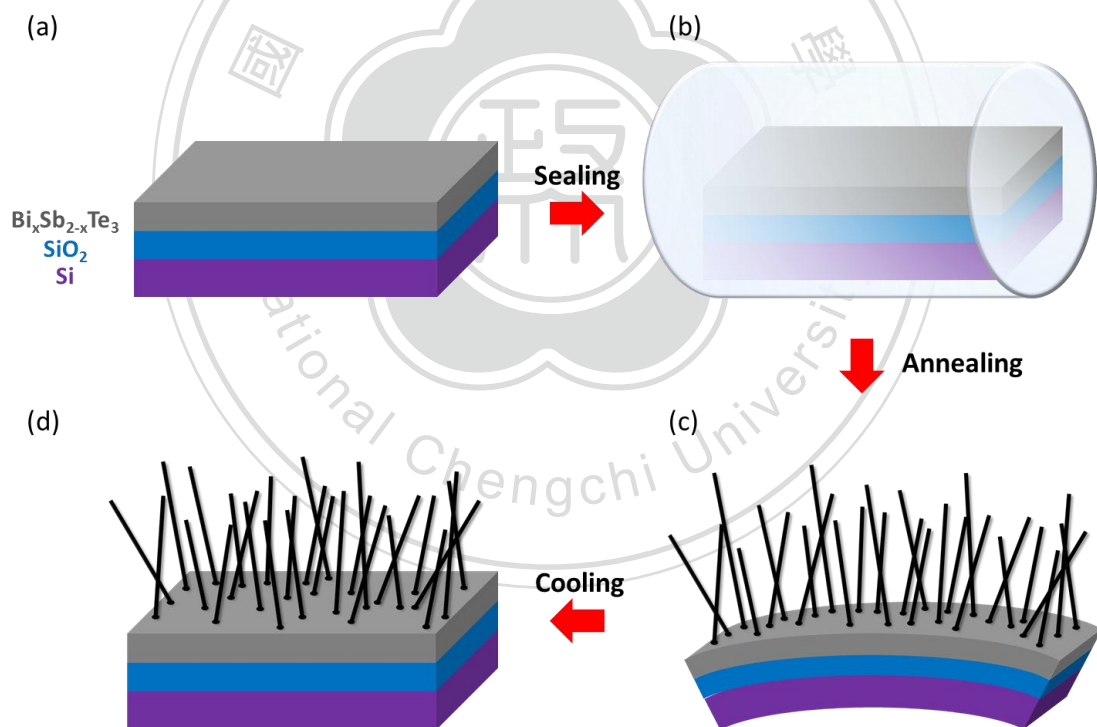
Figure 3.1   Schematic representation of the growth of $Bi_xSb_{2-x}Te_3$ nanowires by stress-induce method. (a) Deposit $Bi_xSb_{2-x}Te_3$ thin films on SiO_2/Si substrates by using pulsed laser deposition system. (b) Seal the films in a vacuumed quartz tube. (c) Anneal the films at 350~500 ℃ for 5~21 days (d) Completion of $BiS_xb_{2-x}Te_3$ nanowires growth.

3.1 Experimental equipment and techniques

X-ray diffraction (XRD)

X-ray diffraction (XRD) is a common technique for analyzing the crystal structure of materials. Now consider a monochromatic X-ray beam with wavelength λ at an incident angle θ is incident in a crystalline material that the spacing between diffracting planes of the material is d. The path difference of the scattered X-ray by two nearby diffracting plane equals to $2d\sin\theta$. The scattered X-ray interfere constructively when the path difference of the scattered X-ray equals to an integer multiple of the wavelength. This leads to Bragg law $n\lambda = 2d\sin\theta$. By analyzing the X-ray diffraction pattern, we can identify the structure of materials.
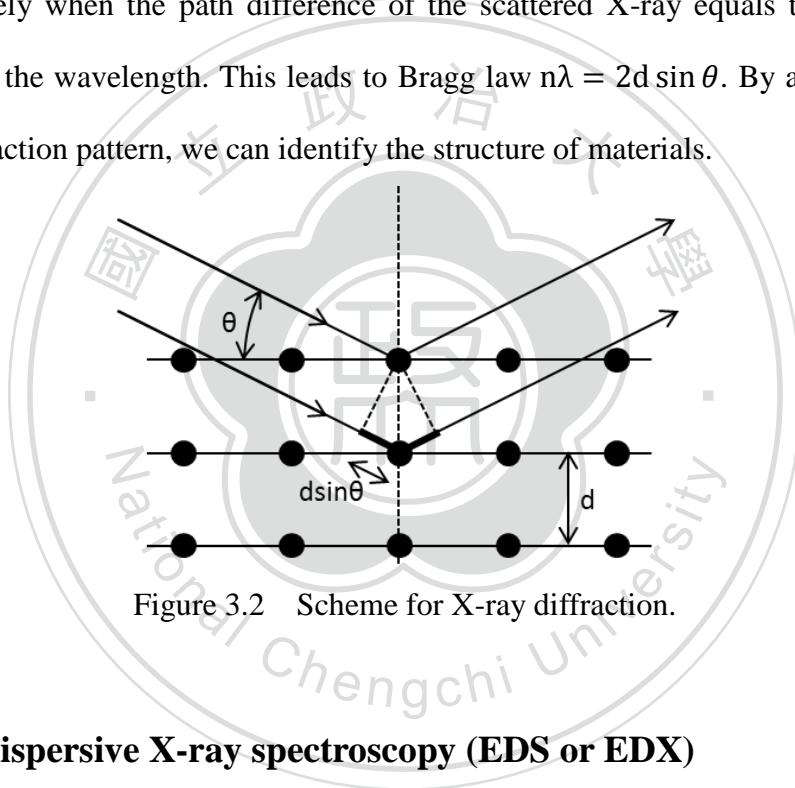
Figure 3.2   Scheme for X-ray diffraction.

Energy-dispersive X-ray spectroscopy (EDS or EDX)

Energy-dispersive X-ray spectroscopy (EDS or EDX) is an analytical technique used for the elemental analysis or chemical characterization of a sample. It relies on the investigation of an interaction of some source of X-ray excitation and a sample. Its characterization capabilities are due in large part to the fundamental principle that each element has a unique atomic structure allowing unique set of peaks on its X-ray spectrum To stimulate the emission of characteristic X-rays from a specimen, a high-energy beam of charged particles such as electrons or protons, or a beam of

X-rays, is focused into the sample being studied. The incident beam may excite an electron in an inner shell, ejecting it from the shell while creating an electron hole where the electron was. An electron from an outer, higher-energy shell then fills the hole, and the difference in energy between the higher-energy shell and the lower energy shell may be released in the form of an X-ray. As the energy of the X-rays are characteristic of the difference in energy between the two shells, and of the atomic structure of the element from which they were emitted, this allows the elemental composition of the specimen to be measured.

Pulsed laser deposition (PLD)

Pulsed laser deposition is a technique for depositing thin film or making nanoparticle. To deposit thin film, a high power pulsed laser is focused in a vacuum chamber and hit the target. The material which is to be deposited then be vaporized from the target and form a thin film on the substrate. Substituting substrate into liquid nitrogen-cooled copper plate and following a similar procedure in background gas then it can get nanoparticle instead of thin film.

Figure 3.3 Pulsed laser deposition system for nanoparticles and thin film fabrication.

Scanning electron microscope (SEM)

A scanning electron microscope (SEM) is a type of electron microscope that images a sample by scanning it with a beam of electrons. Electron beam is emitted from an electron gun and be focused by condenser lenses to a spot and interacts with the sample. The energy exchange between the electron beam and the sample results in emission of secondary electrons by inelastic scattering and the emission of electromagnetic radiation, the reflection of high-energy electrons by elastic scattering, each of which can be detected by specialized detectors. The signal then is converted into image and display on the monitor.

Transmission electron microscopy (TEM)

Transmission electron microscopy (TEM) is a microscopy technique whereby a beam of electrons is transmitted through an ultra-thin specimen, interacting with the specimen as it passes through. An image is formed from the interaction of the electrons transmitted through the specimen; the image is magnified and focused onto an imaging device, such as a fluorescent screen, on a layer of photographic film, or to be detected by a sensor such as a CCD camera.
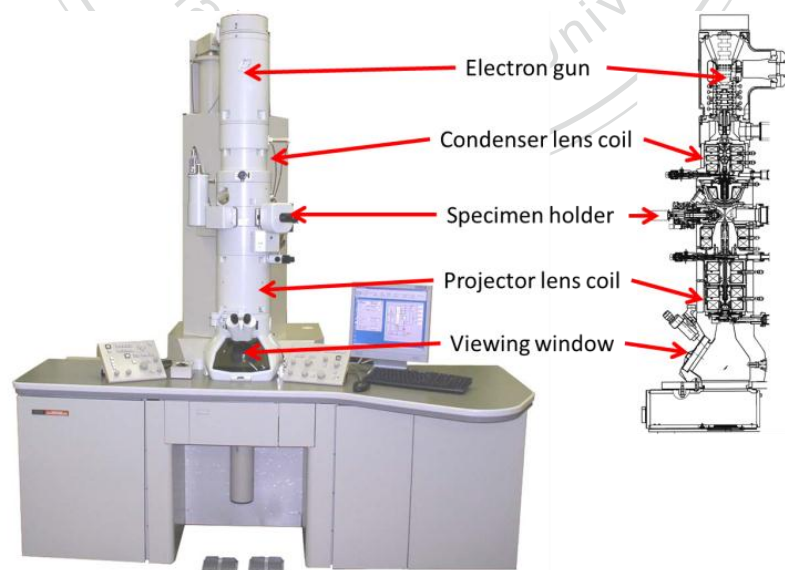
Figure 3.4   Exterior view of TEM and cross section of column.

Selected area diffraction (SAD)

In a TEM, a thin crystalline specimen is subjected to a parallel beam of high-energy electrons. Because the wavelength of high-energy electrons is a few thousandths of a nanometer and the spacing between atoms in a solid is about a hundred times larger, the atoms act as a diffraction grating to the electrons, which are diffracted. That is, some fraction of them will be scattered to particular angles, determined by the crystal structure of the sample, while others continue to pass through the sample without deflection. As a result, the image on the screen of the TEM will be a series of spots—the selected area diffraction pattern, SADP, each spot corresponding to a satisfied diffraction condition of the sample's crystal structure.

3.2 Target preparation

To prepare the target of the pulsed laser deposition system, Bi_2Te_3 and Sb_2Te_3 powders were mixed by a particular ratio. The mixed powder is sealed into a vacuumed quartz tube The tube with the powder inside was put into the furnace and heated up to 750℃. The melting point of Bi_2Te_3 and Sb_2Te_3 are 585℃ and 580℃ respectively Temperature was kept at 750℃ for a few hours to make sure the Bi_2Te_3 and Sb_2Te_3 were form into $Bi_xSb_{2-x}Te_3$ compound. The tube containing the melting compound was slowly cool down to room temperature and formed a bulk. The bulk was cut into ingot. The structure and the composition of the ingot were checked by the XRD and EDX respectively.
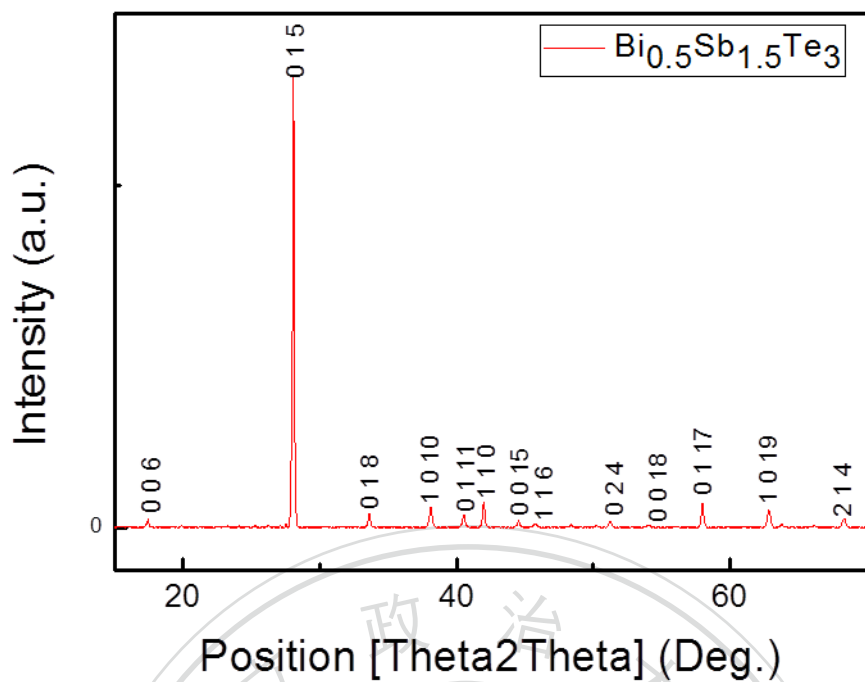
Figure 3.5   X-Ray diffraction pattern of $Bi_{0.5}Sb_{1.5}Te_3$ ingot.
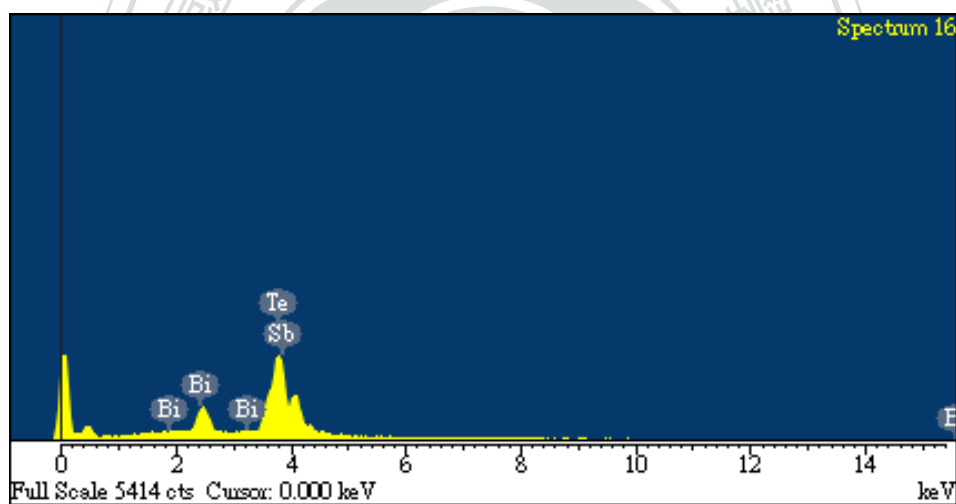
Figure 3.6   EDX spectrum of $Bi_{0.5}Sb_{1.5}Te_3$ ingot.

Table 3.1   The weight percentage and atomic percentage of the $Bi_{0.5}Sb_{1.5}Te_3$ ingot.

Element	Weight%	Atomic%
Bi	14.48	9.24
Sb	28.4	31.09
Te	57.13	59.68
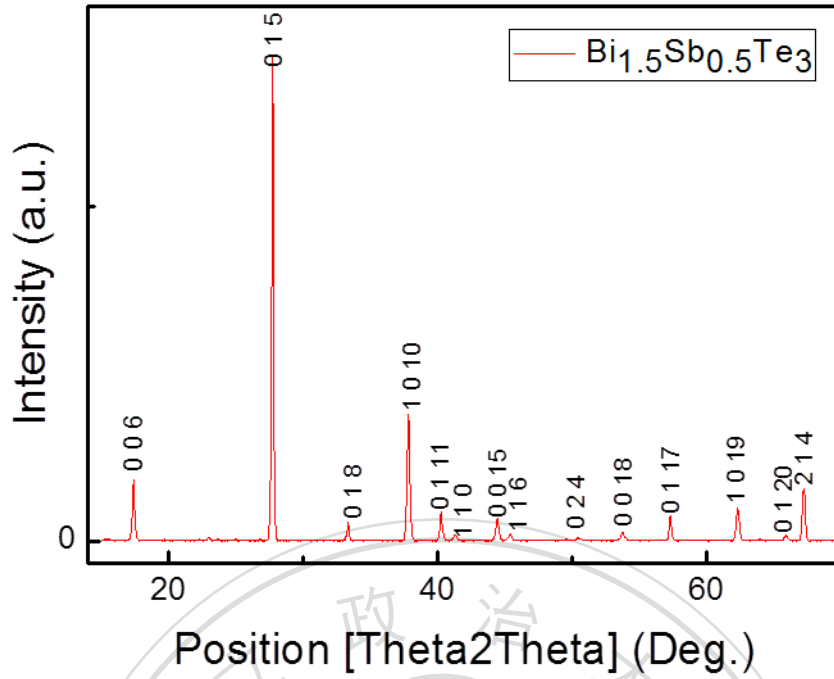
Figure 3.7   X-Ray diffraction pattern of $Bi_{1.5}Sb_{0.5}Te_3$ ingot.
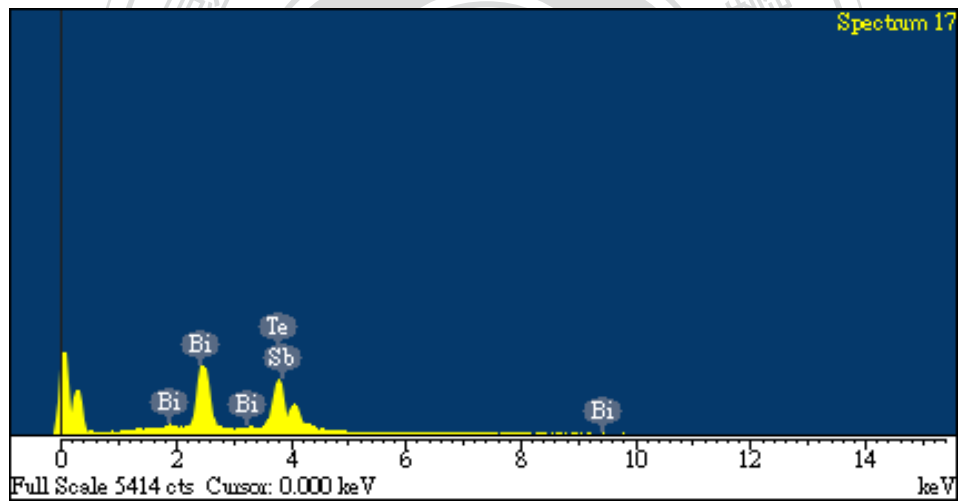
Figure 3.8   EDX spectrum of $Bi_{1.5}Sb_{0.5}Te_3$ ingot.

Table 3.2   The weight percentage and atomic percentage of the $Bi_{1.5}Sb_{0.5}Te_3$ ingot.

Element	Weight%	Atomic%
Bi	40.83	29.51
Sb	8.04	9.97
Te	51.23	60.52

3.3 Film deposition

Cut the silicon (Si) wafer with 300nm silicon oxide ($SiO_{2)}$ into $9\sim600mm^2$ rectangular SiO_2/Si substrates. Substrates were cleaned by using acetone, isopropyl alcohol and deionized water in ultrasonic bath for 10 minute each, respectively.

Stick the SiO_2/Si substrates on the substrate holder and fix the target on the target holder of the pulsed laser deposition system (PLD). The distance between the target and the substrate was 8 cm. Adjust the laser to focus on the surface of the target. Vacuum the chamber by rotary pump and cryopump to the pressure lower than 5.0×10^{-7} torr. Use different power and different frequency of the laser to hit the target for a period of time at room temperature. The total thickness of the formed $Bi_xSb_{2-x}Te_3$ films were ranged from few tens of nanometer to few hundreds of nanometers. The composition of the film is confirm by the EDX
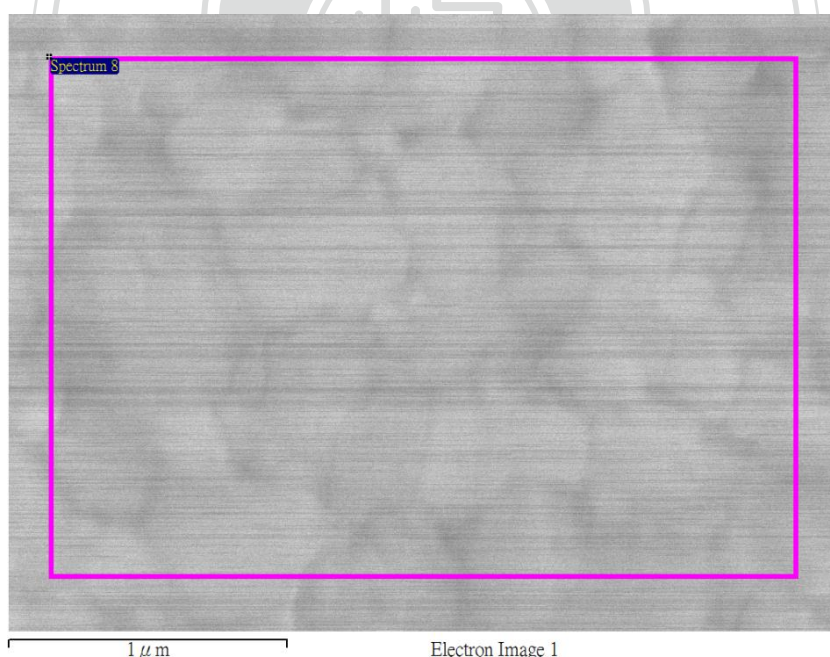
Figure 3.9　SEM image of $Bi_{0.5}Sb1_{1.5}Te_3$ thin film that deposited for 1 hour. The power and the frequency of the laser are 170mJ and 10Hz respectively. The rectangular shows the corresponding area of EDX analysis.
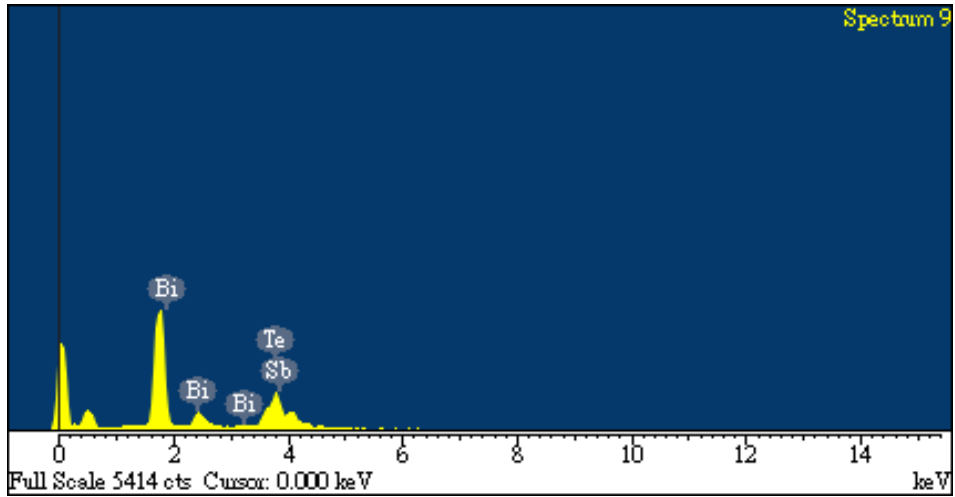
Figure 3.10　EDX spectrum of $Bi_{0.5}Sb_{1.5}Te_3$ film.

Table 3.3　The weight percentage and atomic percentage of the $Bi_{0.5}Sb_{1.5}Te_3$ film.

Element	Weight%	Atomic%
Bi	15.00	9.59
Sb	27.86	30.57
Te	57.14	59.83
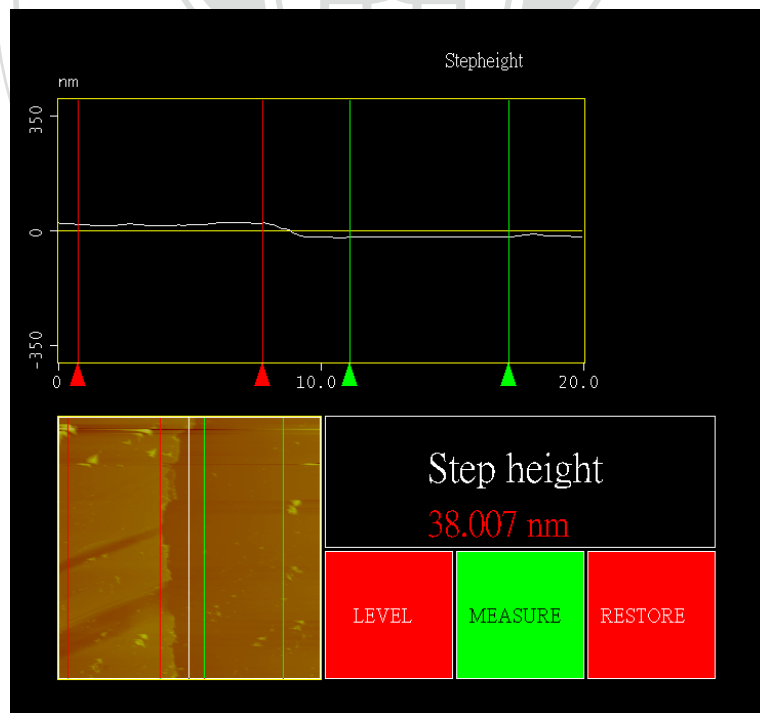
Figure 3.11 AFM analysis shows that the thickness of the film is about 38nm.
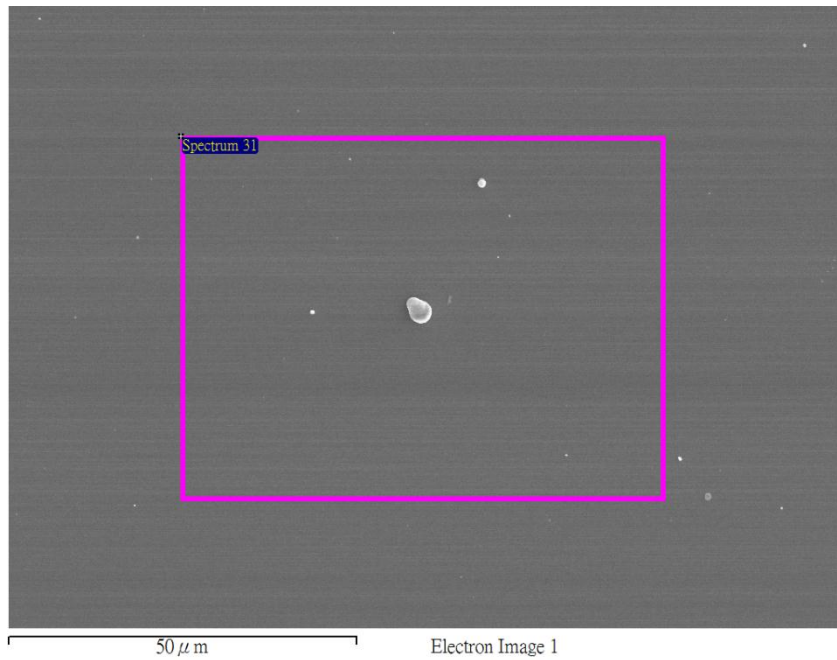
Figure 3.12 SEM image of $Bi_{1.5}Sb_{0.5}Te_3$ thin film that deposited for 5 min. The power and the frequency of the laser are 160mJ and 30Hz respectively. The rectangular shows the corresponding area of EDX analysis.
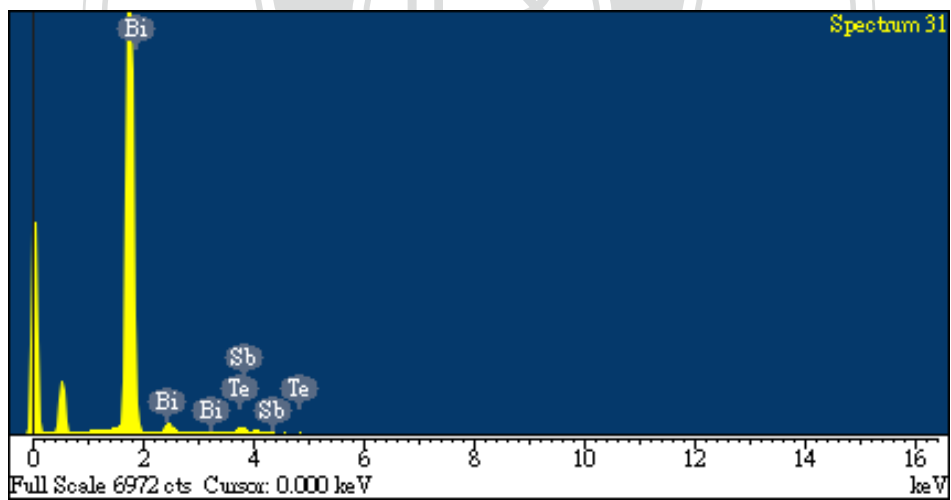
Figure 3.13 EDX spectrum of $Bi_{1.5}Sb_{0.5}Te_3$ film.

Table 3.4 The weight percentage and atomic percentage of the $Bi_{1.5}Sb_{0.5}Te_3$ film.

Element	Weight%	Atomic%
Bi	42.43	30.90
Sb	7.44	9.30
Te	50.13	59.80
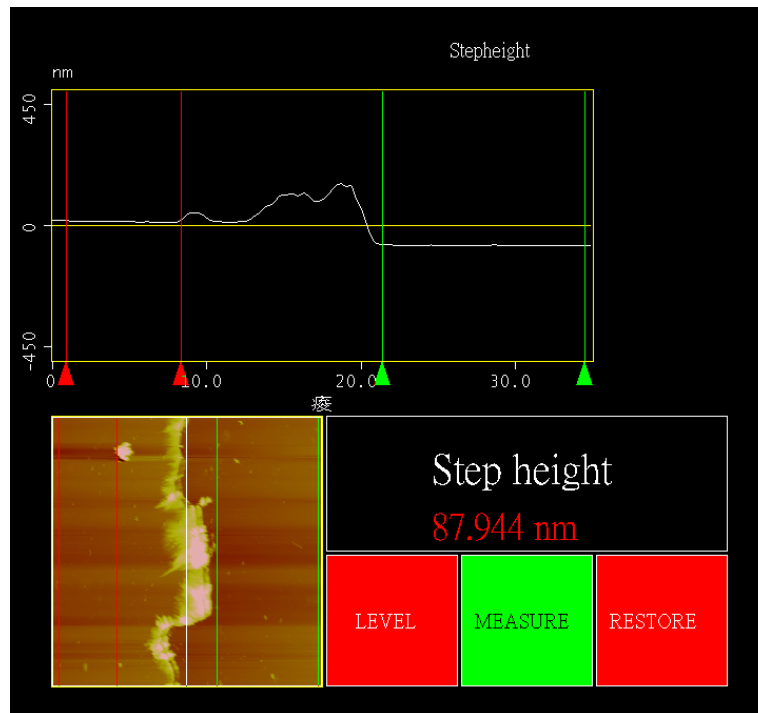
Figure 3.14 AFM analysis shows that the thickness of the film is about 88nm.

3.4 Annealing process

The films were sealed in a vacuumed quartz tube below the pressure of 5×10^{-6} mbar and anneal them at 350~500 ℃ for 5~21 days. The thermal expansion coefficient of the $Bi_xSb_{2-x}Te_3$ film (~13.4×10^{-6}/℃), SiO_2 (0.5×10^{-6}/℃) and Si (2.4×10^{-6}/℃) are different. During the annealing process, the substrate restricted the expansion of the film and put the film under compressive stress. The nanowires then grew from the film in order to release the compressive stress. The films were cooled down in air. Scanning electron microscope (SEM) and optical microscope (OM) were used to observe the nanowire.
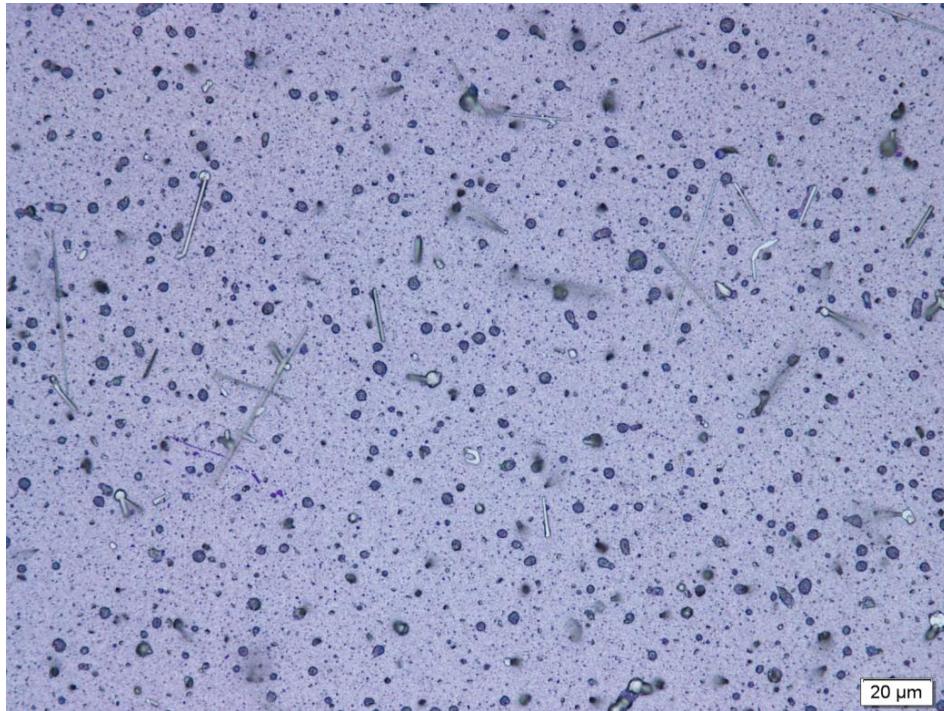
Figure 3.15   OM image of the $Bi_{0.5}Sb_{1.5}Te_3$ thin film after annealing at 350 ℃ for 21

days.

Figure 3.16   Side view SEM image of $Bi_{0.5}Sb_{1.5}Te_3$ film after annealing at 350 ℃

for 21 days.
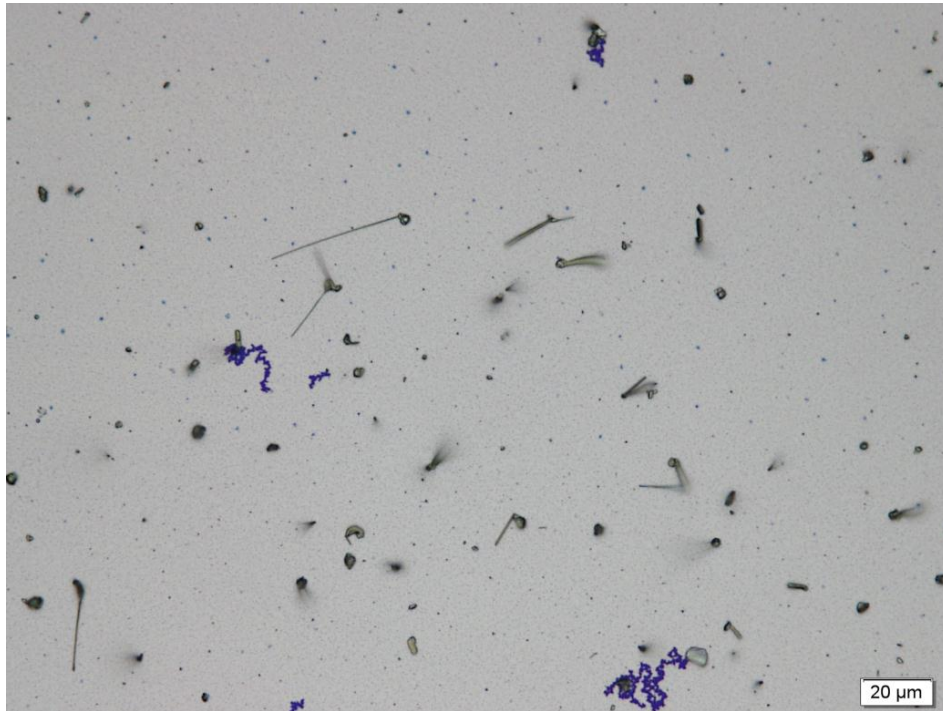
Figure 3.17　OM image of the $Bi_{1.5}Sb1_{0.5}Te_3$ thin film after annealing at 490 ℃ for 5

days.

Figure 3.18　Side view SEM image of $Bi_{1.5}Sb1_{0.5}Te_3$ film after annealing at 490 ℃

for 5 days.

3.5 Analysis results

In order to analyze a single nanowire by transmission electron microscopy (TEM), the wire was suspended on a measurement platform so that electron beam can penetrate the wire. The wire is divided into three parts. The end close to the heater is defined as top part. The end away from the heater is defined as bottom part. Between the top and the bottom is the middle part. To see if the wire is well crystalized or not and the growth orientation of the nanowire, selected area diffraction (SAD) was taken. To see the distribution of the bismuth, antimony and telluride in the wire, EDX line-scan profile was taken. To know the ratio between the three element EDX point scan has been done.

Nanowire No.1
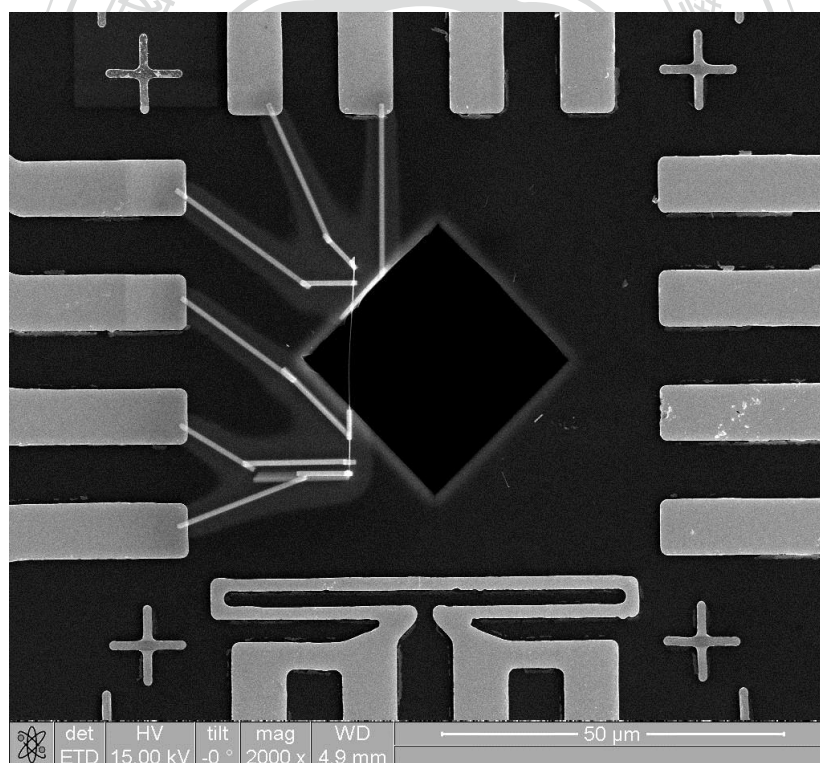
Figure 3.19   SEM image of a suspend nanowire No.1 which grown from $Bi_{0.5}Sb_{1.5}Te_3$ film after annealing at 500 ℃ for 5 days. The nanowire is 150 nm in diameter. The electrodes had already deposited by the FIB.
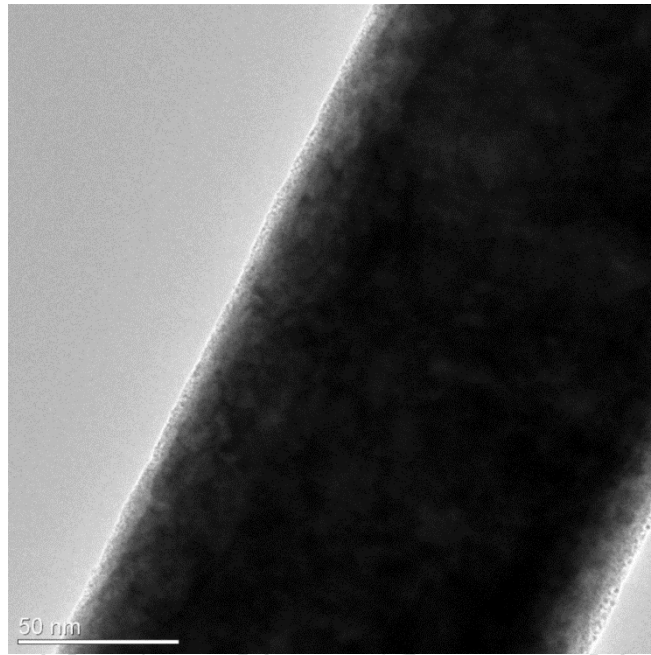
Figure 3.20　TEM image of the nanowire No. 1.
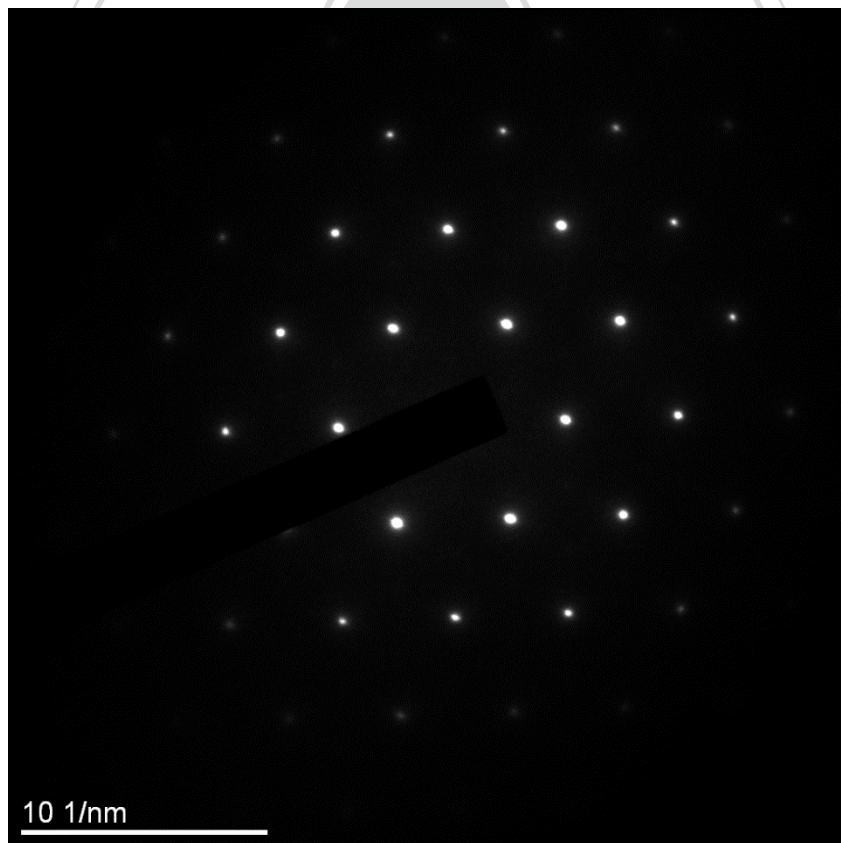
Figure 3.21　Selected area diffraction pattern of the nanowire No. 1.
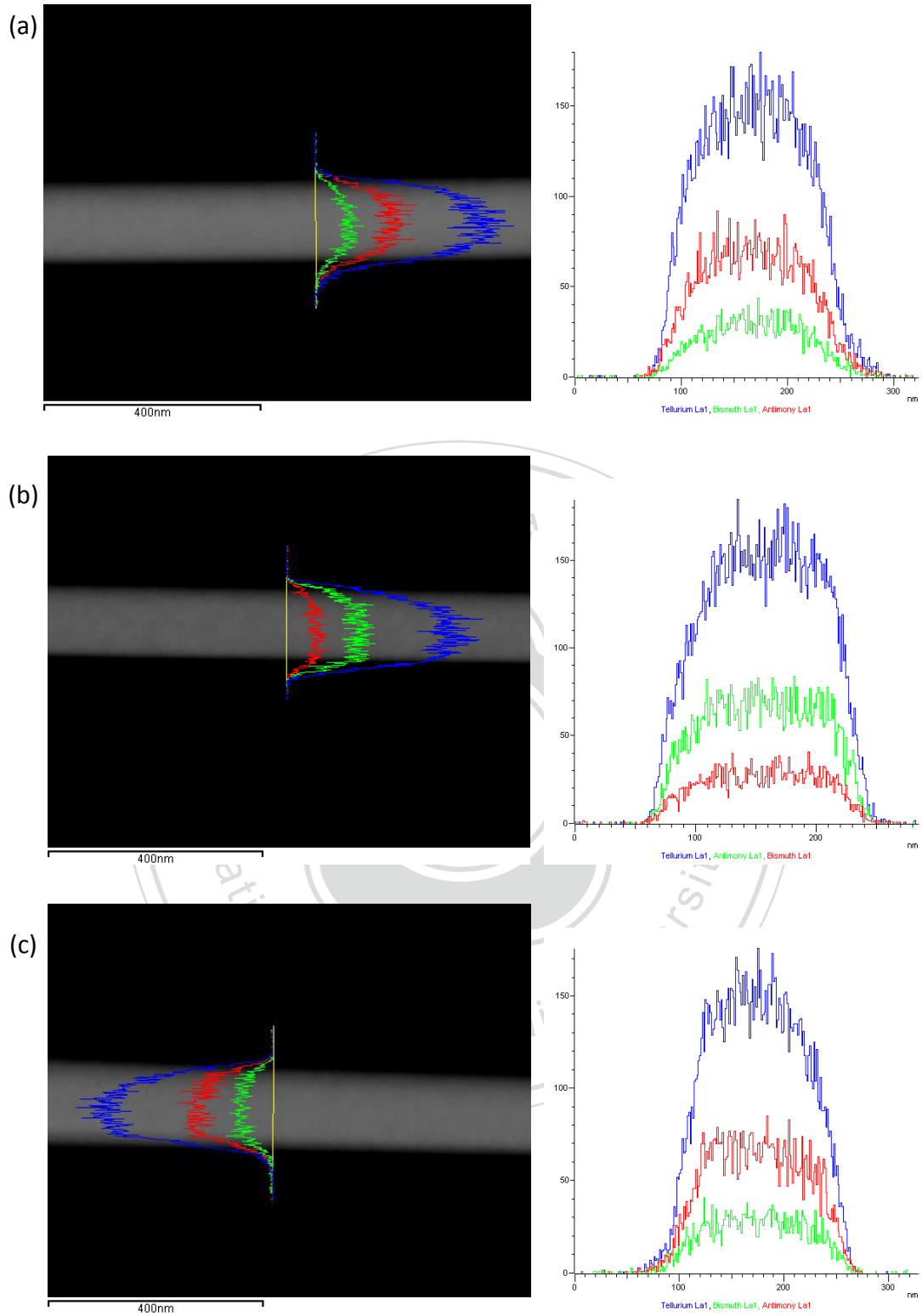
Figure 3.22   The scanning TEM image of (a) top (b) middle (c) bottom part of the nanowire No.1. The EDX line-scan profile show that Bismuth, antimony and telluride homogeneously distributed through the nanowire.
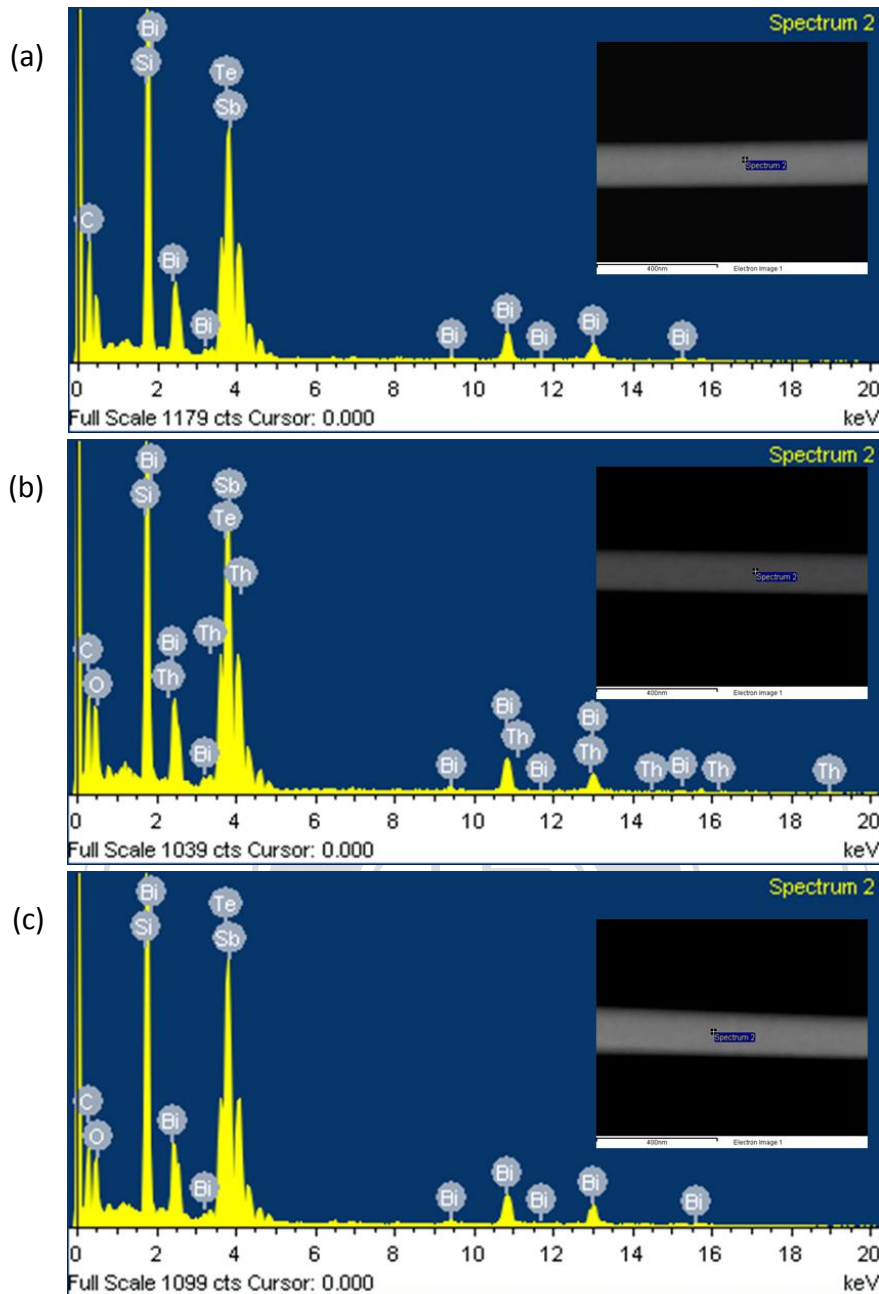
Figure 3.23   EDX point-scan spectrum of the (a) top (b) middle (c) bottom part of

the nanowire No.1. The inset shows the corresponding point.

Table 3.5   Weight percentage and atomic percentage of three parts of the nanowire

Element	Atomic%			Atom number		
	Top	Middle	Bottom	Top	Middle	Bottom
Bi	13.13	13.20	12.87	0.62	0.62	0.62
Sb	29.53	28.88	28.79	1.38	1.38	1.38
Te	57.52	57.92	58.34	2.71	2.71	2.80

Nanowire No.2
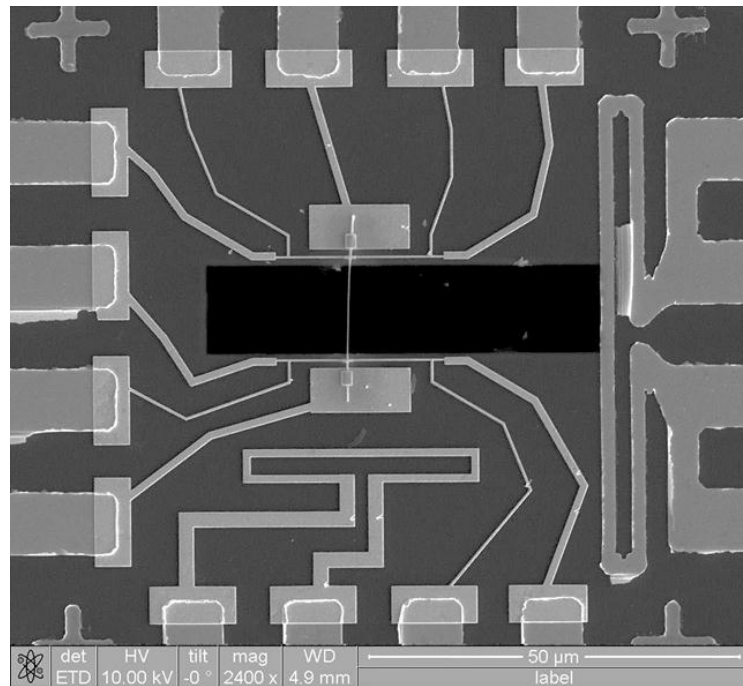
Figure 3.24   SEM image of a suspend nanowire No.2 which grown from $Bi_{1.5}Sb_{0.5}Te_3$ film after annealing at 490 ℃ for 5 days. The nanowire is 220 nm in diameter.
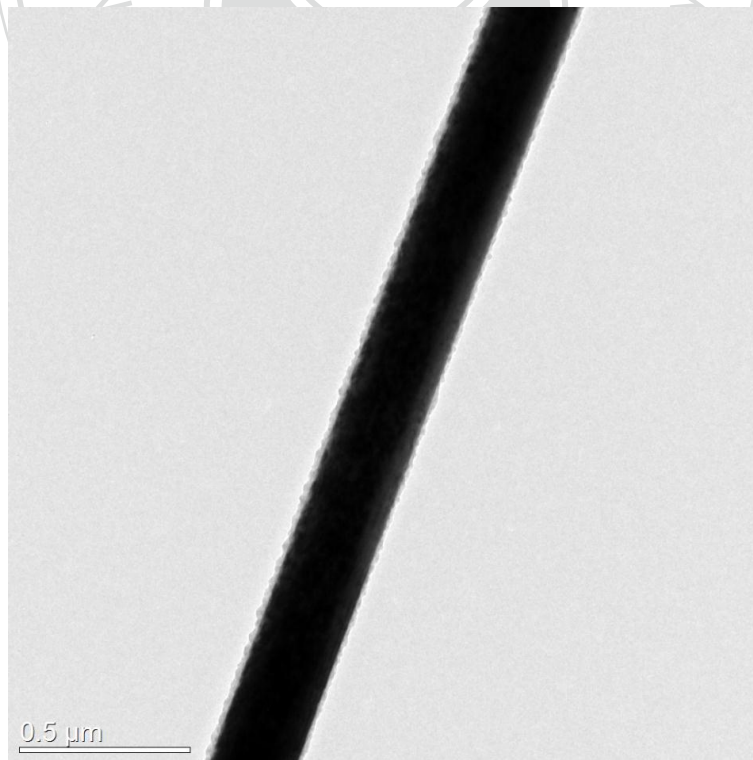
Figure 3.25   TEM image of the nanowire No. 2.
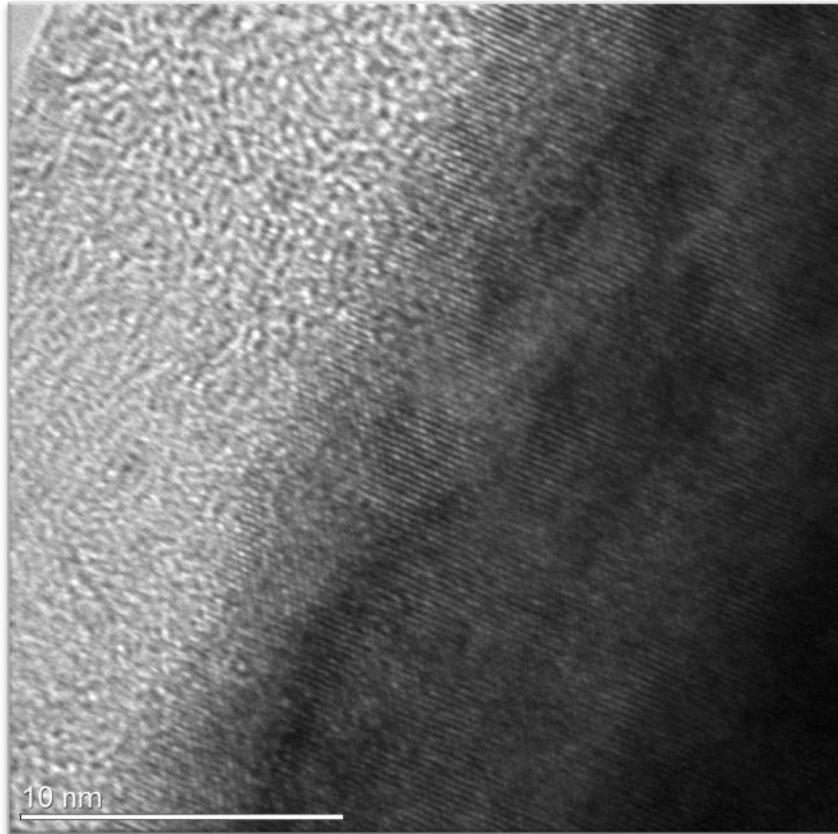
Figure 3.26　TEM image of the nanowire No. 2.
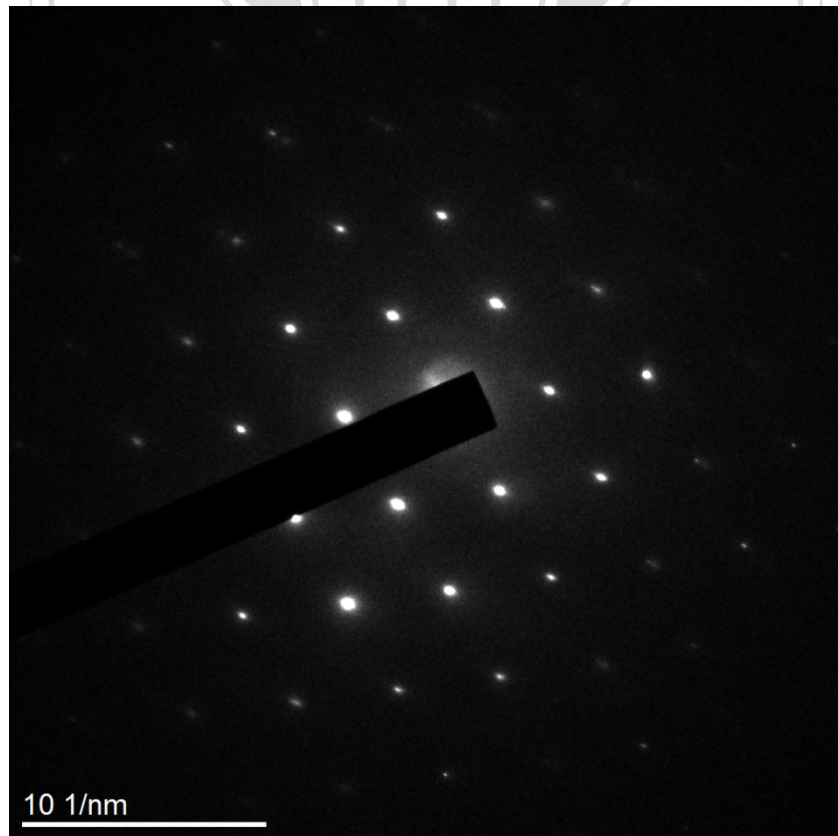
Figure 3.27　Selected area diffraction pattern of the nanowire No. 2.
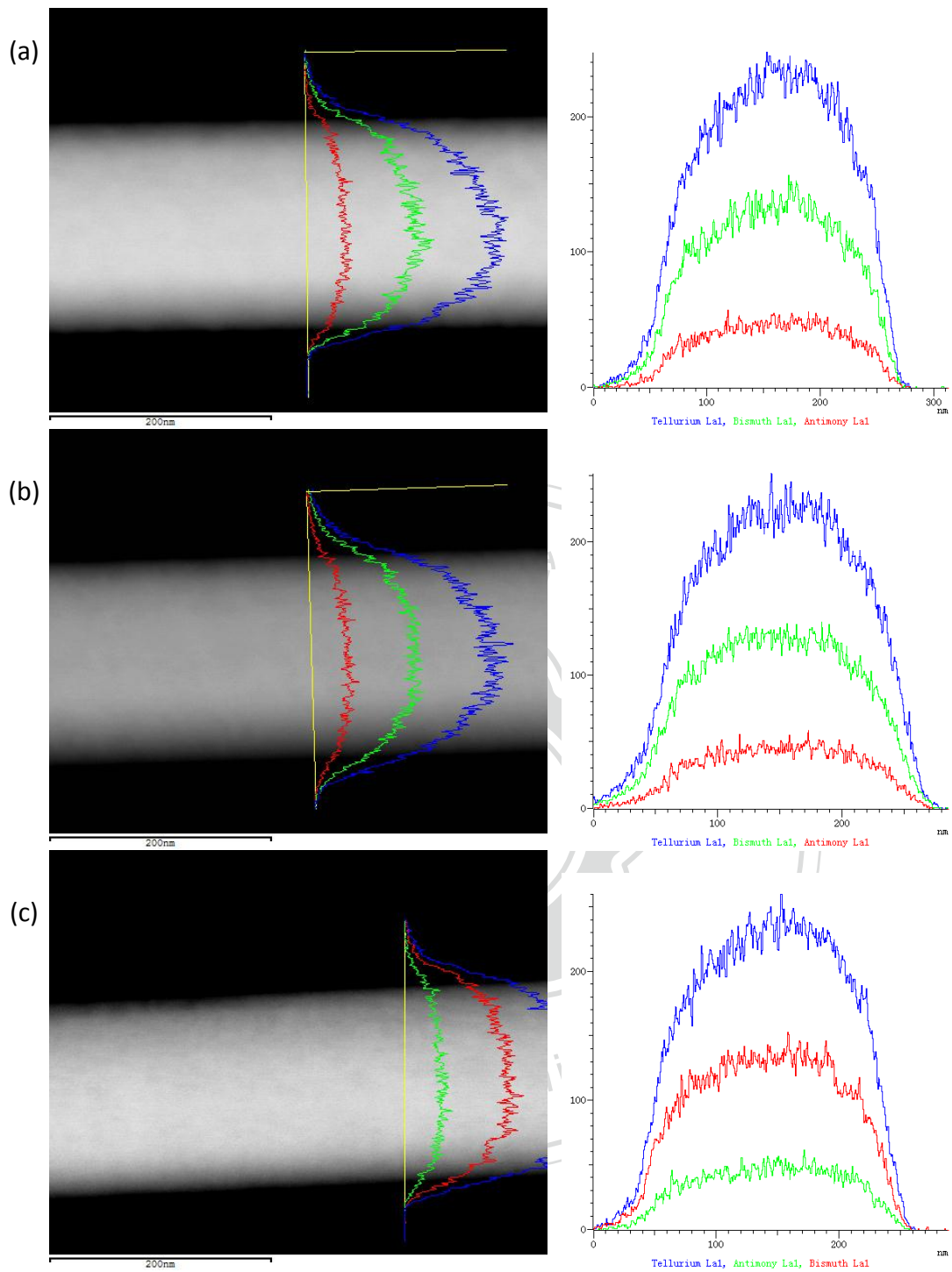
Figure 3.28   The scanning TEM image of (a) top (b) middle (c) bottom part of the nanowire No.2. The EDX line-scan profile show that Bismuth, antimony and telluride homogeneously distributed through the nanowire.
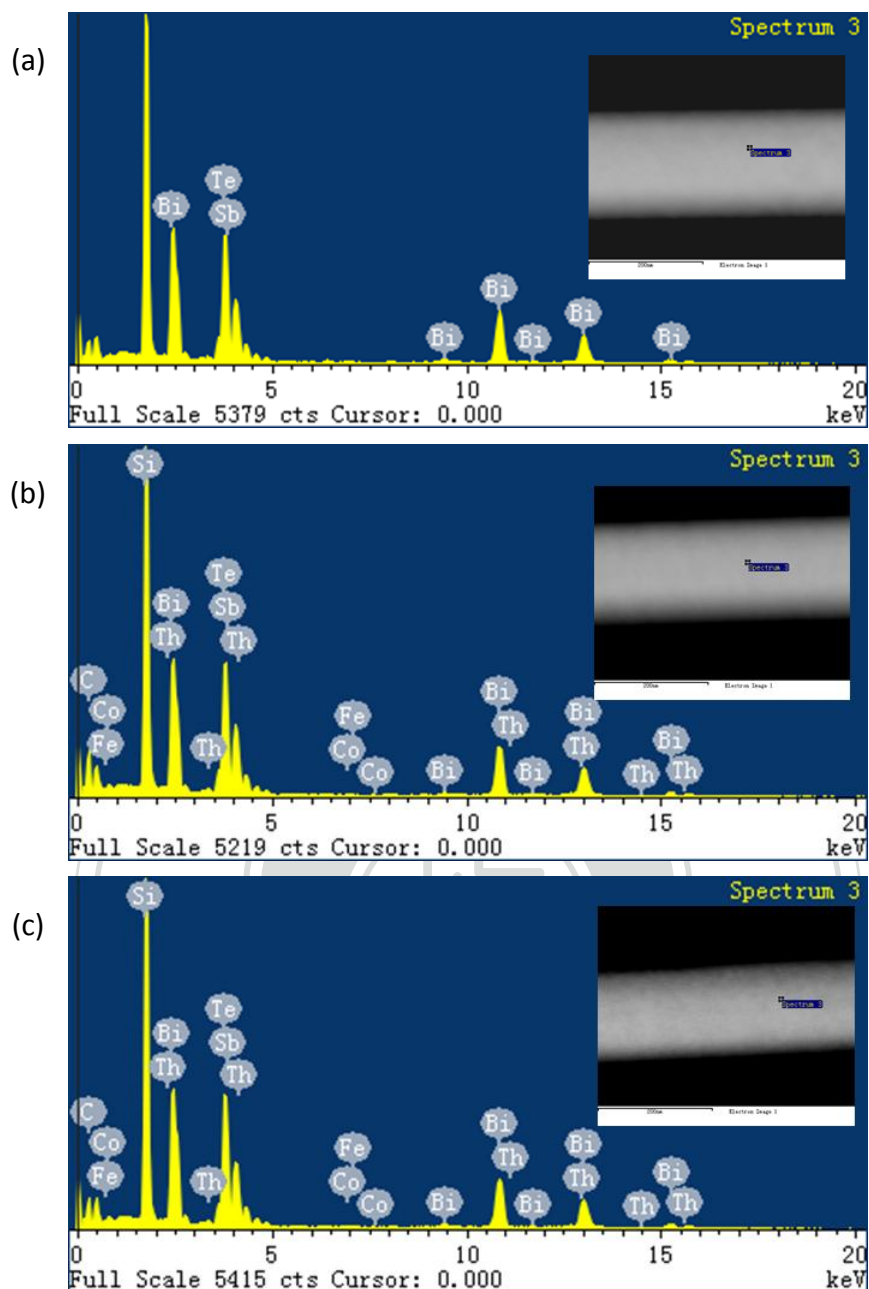
Figure 3.29　EDX point-scan spectrum of the (a) top (b) middle (c) bottom part of

the nanowire No.2. The inset shows the corresponding point.

Table 3.6　Weight percentage and atomic percentage of three parts of the nanowire

Element	Atomic%			Atom number		
	Top	Middle	Bottom	Top	Middle	Bottom
Bi	37.54	37.34	37.46	1.66	1.66	1.66
Sb	7.64	7.74	7.57	0.34	0.34	0.34
Te	54.83	54.92	54.97	2.43	2.44	2.44

Chapter 4

Thermoelectric property measurements of nanowires

Introduction

This chapter shows that how to measure the thermoelectric properties and the measurement result. In order to applied 3ω method to measure the thermal conductivity, nanowire was suspended on the measurement platform to allow the temperature fluctuation. In order to measure the thermoelectric properties, electrodes, heater and thermometers were fabricated on the measurement platform. Secstion4.1 introduces the acquired equipment and techniques. Section 4.2 shows how to fabricate the measurement platform and suspend a wire on it. Section 4.4 shows how to measure the thermoelectric properties of the nanowire. Section 4.5 shows the measurement result.

4.1 Experimental equipment and techniques
Photolithography

Photolithography is a process used in microfabrication to selectively remove parts of a thin film or the bulk of a substrate. It uses light to transfer a pattern from a mask to a light-sensitive chemical photoresist on the substrate. A series of chemical treatments then either engraves the exposure pattern into, or enables deposition of a new material in the desired pattern upon, the material underneath the photo resist.

Dry etch

Dry etching refers to the removal of material, typically a masked pattern of semiconductor material, by exposing the material to a bombardment of ions that dislodge portions of the material from the exposed surface. Unlike with many of the wet chemical etchants used in wet etching, the dry etching process typically etches directionally or anisotropically.

Wet etch

The wafer is immersed in a bath of etchant, which must be agitated to achieve good process control. Etching a (100) silicon surface through a rectangular hole in a masking material creates a pit with flat sloping <111>-oriented sidewalls and a flat <100>-oriented bottom. The <111>-oriented sidewalls have an angle to the surface of the wafer of: $\tan^{-1}\sqrt{2} = 54.7°$. If the original rectangle was a perfect square, the pit when etched to completion displays a pyramidal shape.

Lift-off process [7]

A polymer resist layer is patterned first by optical or e-beam lithography. Metallic thin film is then deposited onto the patterned resist layer. A wet chemical solution dissolves the resist layer, which also lifts off the metallic thin film on top of resist layer from the substrate. Only the metallic film deposited through the resist pattern opening onto the substrate remains. In this way, the resist pattern is transferred onto the substrate as a metallic pattern of reverse polarity.

Focused ion beam (FIB)

FIB systems operate in a similar fashion to a scanning electron microscope (SEM) except, rather than a beam of electrons and as the name implies, FIB systems use a finely focused beam of ions (usually gallium) that can be operated at low beam currents for imaging or high beam currents for site specific sputtering or milling. An FIB can used to deposit material via ion beam induced deposition. FIB-assisted chemical vapor deposition occurs when a gas, such as tungsten hexacarbonyl $(W(CO)_6)$ is introduced to the vacuum chamber and allowed to chemisorb onto the sample. By scanning an area with the beam, the precursor gas will be decomposed into volatile and non-volatile components; the non-volatile component, such as tungsten, remains on the surface as a deposition.

Probe station with micropositioner

A probe station can be used to physically acquire signals from the internal nodes of a semiconductor device. The probe station utilizes manipulators which allow the precise positioning of thin needles on the surface of a semiconductor device. Here, the setup is used for manipulating nanowires. The micropositioner is equip with cat-whisker probe tip and fixed on probe station.

Figure 4.1 Set up of probe station with micropositioner for manipulating nanowire.

Four-point probe method

Current is supplied via a pair of current leads generate a voltage drop across the specimen and also across the current leads themselves. To avoid including that in the measurement, a pair of voltage leads is connected to the specimen. The accuracy of the technique comes from the fact that almost no current flows in the sense wires, so the voltage drop V=RI is extremely low.
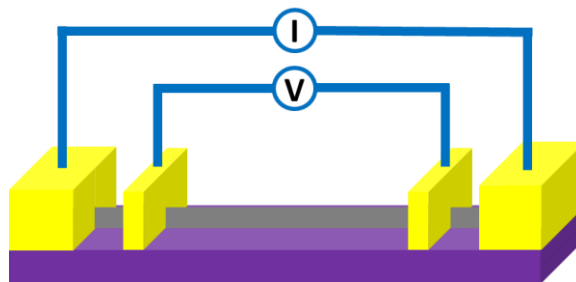
Figure 4.2 Four-probe configuration for measuring the resistivity of a wire.

Resistance thermometer

Resistance thermometer is sensor used to measure temperature by correlating the resistance of the resistance thermometer element with temperature. The temperature dependence of electrical resistance of conductors is to a great degree linear and can be described by the approximation below:

$$\rho(T) = \rho_0[\alpha_0(T - T_0)] \qquad \alpha_0 = \frac{1}{\rho_0}\left[\frac{\delta\rho}{\delta T}\right]_{T=T_0}$$

ρ_0 just corresponds to the specific resistance temperature coefficient at a specified reference value. That of a semiconductor is however exponential:

$$\rho(T) = S\alpha^{\frac{B}{T}}$$

where S is defined as the cross sectional area and α and B are coefficients determining the shape of the function and the value of resistivity at a given temperature.

3ω method for thermal conductivity measurement [8]

In this method, either the specimen itself serves as a heater and at the same time a temperature sensor, if it is electrically conductive and with a temperature-dependent electric resistance. Feeding an ac electric current of the form $I_0 \sin\omega t$ into the specimen creates a temperature fluctuation on it at the frequency 2ω, and accordingly a resistance fluctuation at 2ω. This further leads to a voltage fluctuation at 3ω across the specimen.

Consider a uniform rod- or filament-like specimen in a four-probe configuration as for electrical resistance measurement. The two outside probes are used for feeding an electric current, and the two inside ones for measuring the voltage across the specimen. The specimen in between the two voltage probes is suspended to allow the temperature fluctuation. All the probes have to be highly thermal conductive, to heat sink the specimen at these points to the substrate. The specimen has to be maintained

in a high vacuum and the whole setup is heat shielded to the substrate temperature to minimize the radial heat loss through gas convection and radiation.
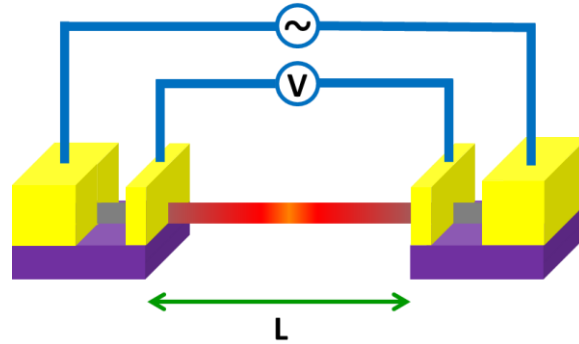
Figure 4.3   Illustration of the four-probe configuration for measuring the specific heat and thermal conductivity of a wire.

In such a configuration and with an ac electrical current of the form $I_0 \sin \omega t$ passing through the specimen, the heat generation and diffusion along the specimen can be described by the following partial differential equation and the initial and boundary conditions:

$$\rho C_p \frac{\partial}{\partial t} T(x,t) - \kappa \frac{\partial^2}{\partial x^2} T(x,t) = \frac{I_0^2 \sin \omega t}{LS} [R + R'(T(x,t) - T_0)] \qquad (4.1)$$

$$\begin{cases} T(0,t) = T_0 \\ T(L,t) = T_0 \\ T(x,-\infty) = T_0 \end{cases} \qquad (4.2)$$

where C_p, κ, R, and ρ are the specific heat, thermal conductivity, electric resistance and mass density of the specimen at the substrate temperature T_0, respectively. $R' = (dR/dT)_{T_0}$. L is the length of the specimen between voltage contacts, and S the cross section of the specimen. Let $\Delta(x,t)$ denote the temperature variation from T_0. i.e. $\Delta(x,t) = T(x,t) - T_0$, Equation (3-1-1) and (3-1-2) become

$$\frac{\partial}{\partial t} \Delta(x,t) - \alpha \frac{\partial^2}{\partial x^2} \Delta(x,t) - c \sin^2 \omega t \cdot \Delta(x,t) = b \sin^2 \omega t \qquad (4.3)$$

where $\alpha = \kappa/\rho C_p$ is the thermal diffusivity and $b = I_0^2 R/\rho C_p LS$, $c = I_0^2 R'/\rho C_p LS$

The temperature distribution along the specimen would be:

$$T(x,t) - T_0 = \Delta_0 \sum_{n=1}^{\infty} \frac{[1 - 1(-1)]^n}{2n^3} \times \sin\frac{n\pi x}{L}\left[1 - \frac{\sin(2\omega t + \phi_n)}{\sqrt{1 + \cot^2 \phi_n}}\right] \qquad (4.4)$$

where $\cot\phi_n = 2\omega\gamma/n^2$ and $\Delta_0 = 2\gamma b/\pi = 2I_0^2 R/(\pi\kappa S/L)$ is the maximum dc temperature accumulation at the center of the specimen. $\gamma \equiv L^2/\pi^2\alpha$ is the characteristic thermal time constant of the specimen for the axial thermal process. Δ_0 is only κ dependent. The information of C_p is included in the fluctuation amplitude of the temperature around the dc accumulation.

By solving the partial difference equation, the resistance fluctuation can be expressed as

$$\delta R = R'\Delta_0 \sum_{n=1}^{\infty} \frac{[1 - 1(-1)^n]^2}{2\pi n^4}\left[1 - \frac{\sin(2\omega t + \phi_n)}{\sqrt{1 + \cot^2 \phi_n}}\right] \qquad (4.5)$$

As a product of the total resistance $R + \delta R$ and the current $I_0 \sin\omega t$, the voltage across the specimen contains a 3ω component $V_{3\omega}(t)$. Only taking the n=1 term at low frequencies, the 3ω component can be express as

$$V_{3\omega}(t) \approx -\frac{2I_0^3 LRR'}{\pi^4 \kappa S\sqrt{1 + (2\omega\gamma)^2}}\sin(3\omega t - \phi) \qquad (4.6)$$

The root-mean-square (rms) values of voltage across the specimen contains a 3ω component

$$V_{3\omega} \approx \frac{4I^3 LRR'}{\pi^4 \kappa S\sqrt{1 + (2\omega\gamma)^2}} \qquad (4.7)$$

By fitting the experimental data to this formula, we can get the thermal conductivity κ and thermal time constant γ of the specimen. The specific heat can then be calculated as

$$C_p = \pi^2\gamma\kappa/\rho L^2 \qquad (4.8)$$

4.2 Primary measurement platform fabrication

First, silicon (Si) wafer with Si_3N_4 on the both sides was covered with photoresist by spin coating. Then photoresist was exposed to a rectangular pattern of ultraviolet light. After exposure, soluble photoresist would be developed by the developer. The wafer was then put into the RIE system. The Si_3N_4 without the protection of the photoresist would be etched by the reactive-ion. Next, the wafer is immersed in a bath of sodium hydroxide solution (NaOH). Si that expose to NaOH would be etch and then create cavities. Wafer with Si_3N_4 membranes would be complete after stripping.

Figure 4.4 Schematic representation of making Si_3N_4 membrane: (Step 1) Substrate spin coat with photoresist. (Step 2) Photoresist be exposed to a pattern of ultraviolet light. (Step 3) Soluble photoresist be developed by the developer. (Step 4) Remove Si_3N_4 by dry etch. (Step 5) Create cavities and leave a Si_3N_4 membrane by wet etch. (Step 6) Strip the photoresist.

Lift-off process was used to make the contact pads of the measurement platform. Si wafer with Si_3N_4 membrane was cover with photoresist by spin coating. Then photoresist was exposed to a pattern of contact pads of ultraviolet light. After exposure, soluble photoresist would be developed by the developer. Use the evaporator to deposit Ni/Au and then lift-off the photoresist by acetone. The primary measurement platform would be ready to be used after lift-off.
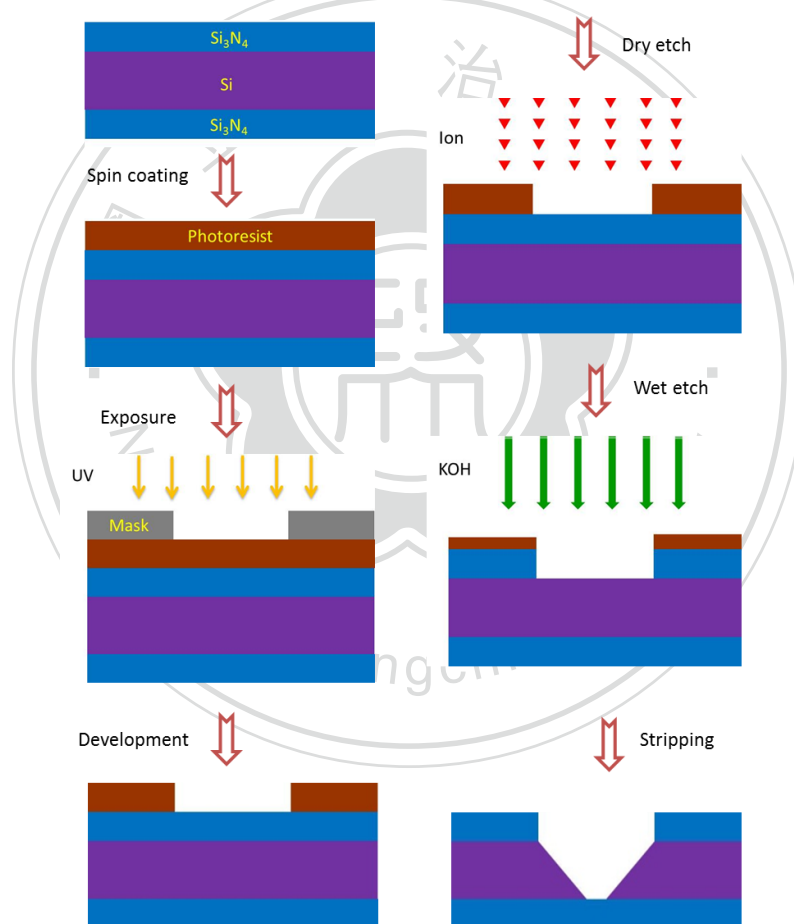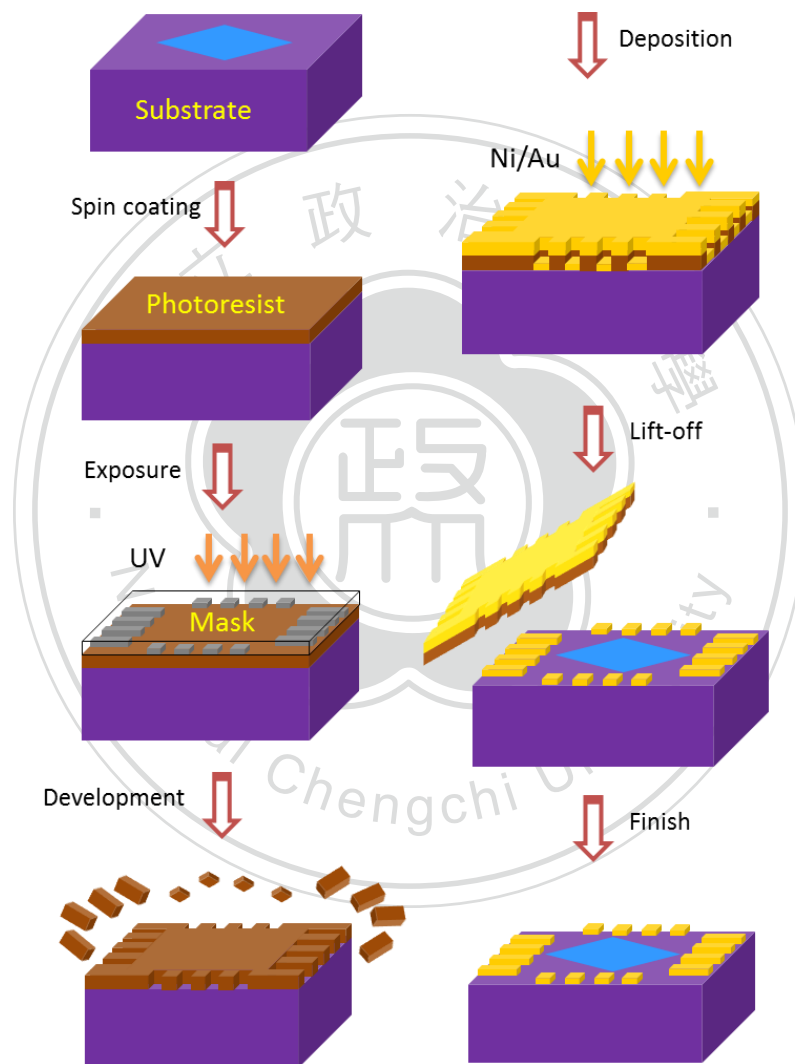

Figure 4.5 Schematic representation of depositing the contact pads: (Step 1) Substrate spin coat with photoresist. (Step 2) Photoresist be exposed to a pattern of ultraviolet light. (Step 3) Soluble photoresist be developed by the developer. (Step 4) Deposit Ni/Au. (Step 5) Lift-off the photoresist.

4.2 Nanowires suspension and completion of measurement platform

Several methods were used to suspend the nanowire and complete the measurement platform.

Method one

First, the primary measurement platform was immersed in the DI water and put into the ultrasonic cleaner. Then the Si_3N_4 membrane was broken by the ultrasonic wave to open a window in the primary measurement platform. Next, the nanowire was picked up by a cat−whisker probe tip which manipulated by a micropositioner under the optical microscope. Then the nanowire was suspended on the on the primary measurement platform and deposit the six electrodes by the FIB.
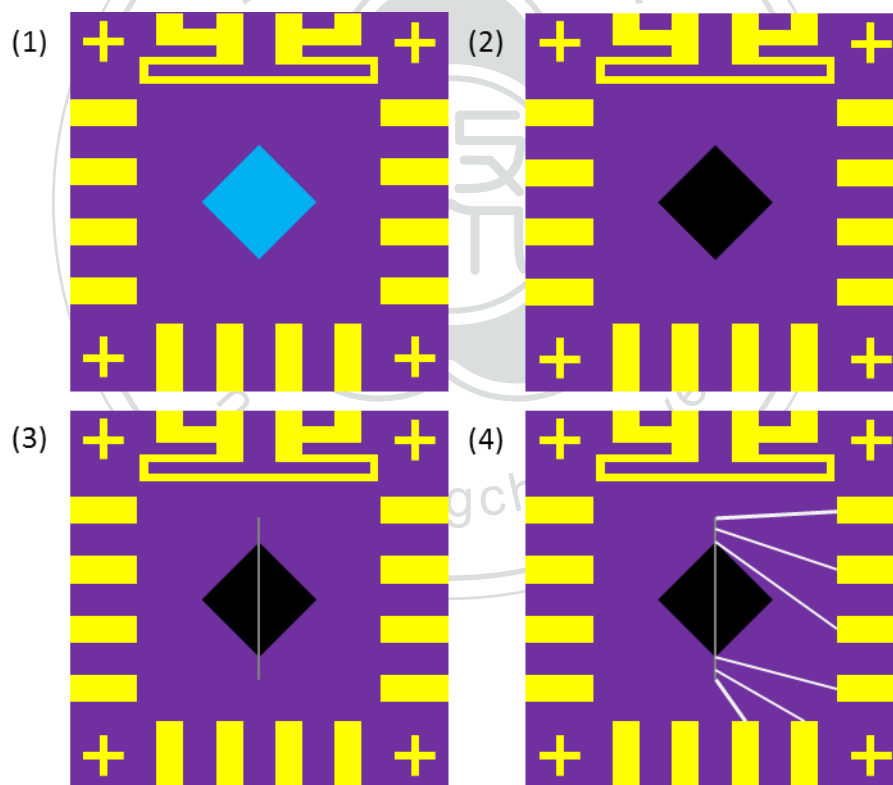
Figure 4.6 Schematic representation of suspend the nanowire and deposit the electrodes by method one. (1)Prepare a primary measurement platform with membrane. (2)Break the membrane by ultrasonic wave. (3)Suspend the wire. (4)Deposit electrode by FIB.
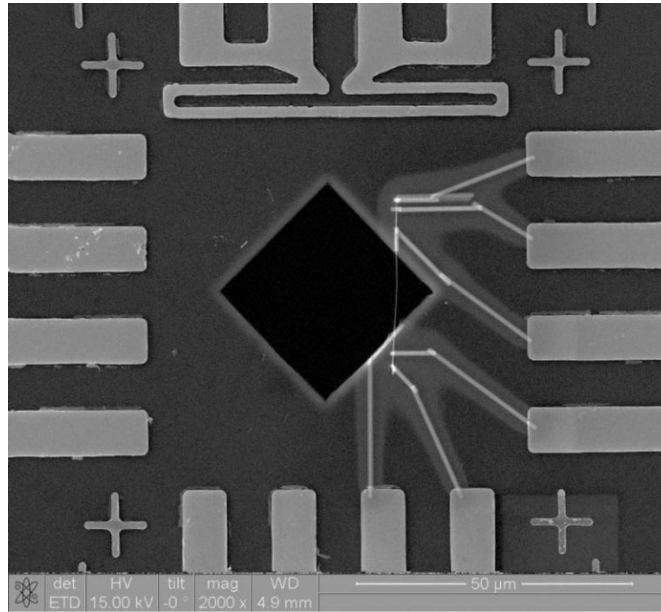
Figure 4.7 SEM image of a suspended nanowire.

Method two

Put the nanowire on the primary measurement platform. Part of the nanowire was laid on the Si_3N_4 membrane. The resistance thermometers, current leads and voltage leads would be made by the electron-beam lithography. Two kind of pattern were used in the measurement. Next, the membrane was etched by the ICP or broke by the tip.
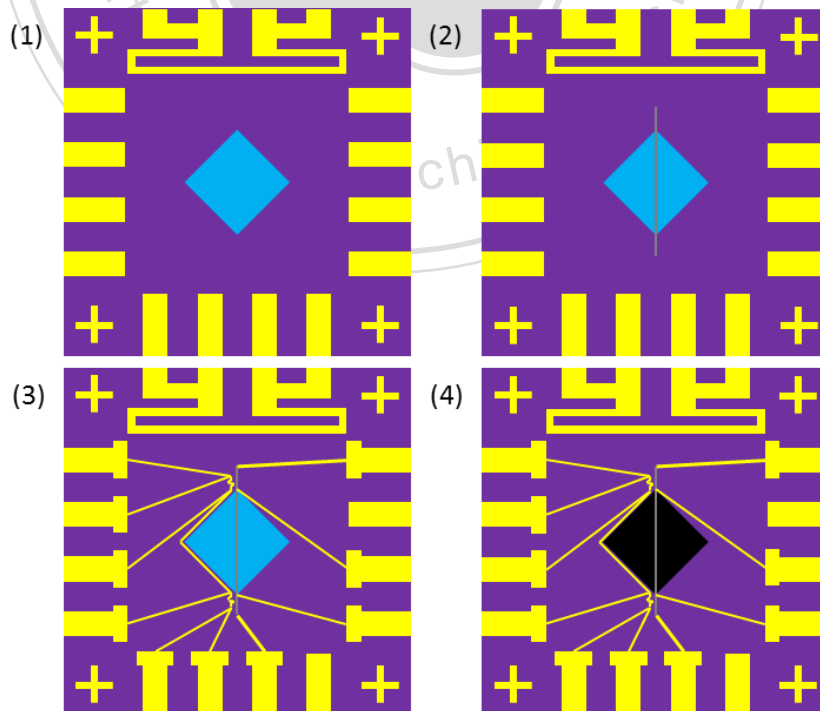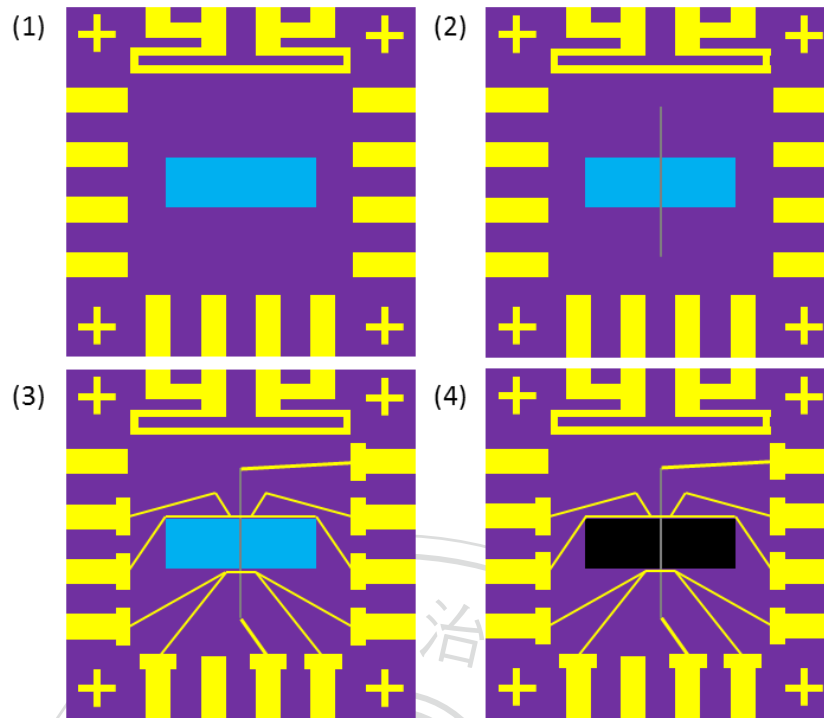
Figure 4.8 Schematic representation of suspend the nanowire and deposit the electrodes by method two. (a) and (b) follow the same procedure but with different pattern. (1)Prepare a primary measurement platform with membrane. (2)Put the wire on the primary measurement platform. (3)Make the thermometer and electrodes by lift-off process. (4)Remove the membrane.
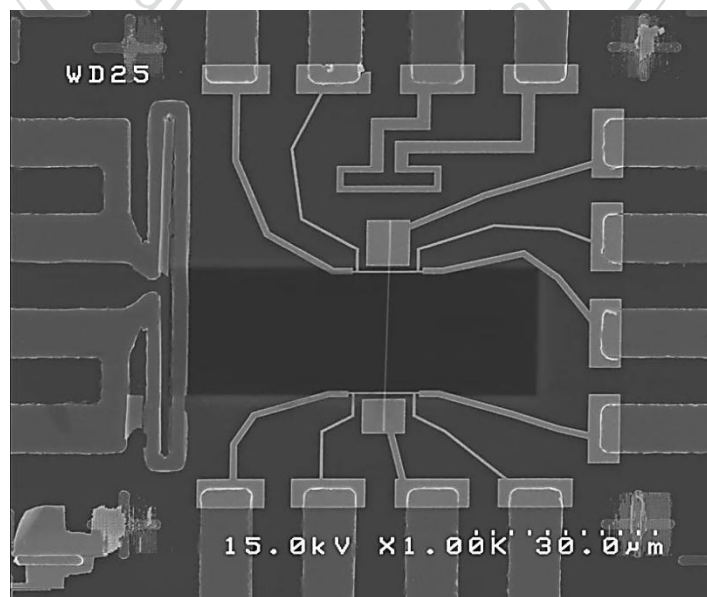
Figure 4.9 SEM top view image of the suspended nanowire.
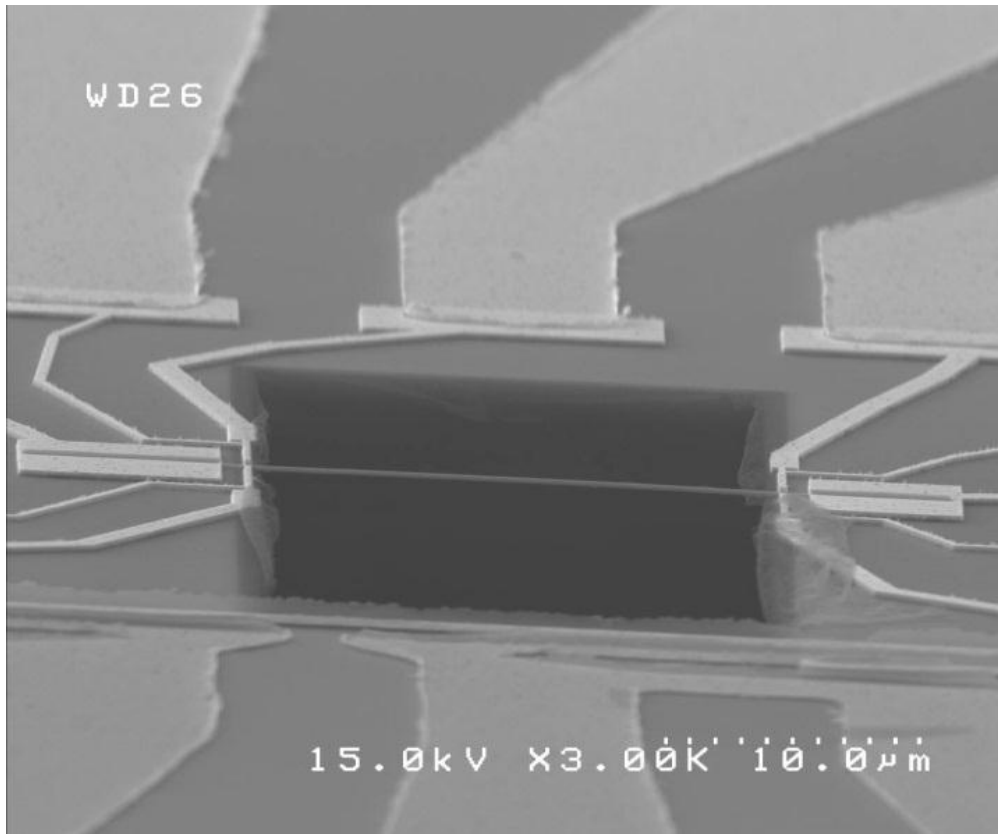
Figure 4.10 SEM tilt view image of the suspended nanowire.

Method three

First, the resistance thermometers, current leads were made by the electron-beam lithography on the primary measurement platform. The Si_3N_4 membrane can break by the ultrasonic wave, reacting ion, plasma or tungsten tip to open a window. Next, the nanowire was hanged across two resistance thermometers with two ends of the wire attach to the current lead. As two electrodes of the thermometer was also the voltage lead of 4-point probes method, the contacts of the nanowire and thermometer would be covered with a layer of platinum which are deposited by the FIB to make a better contact and also the contact of current leads.

39
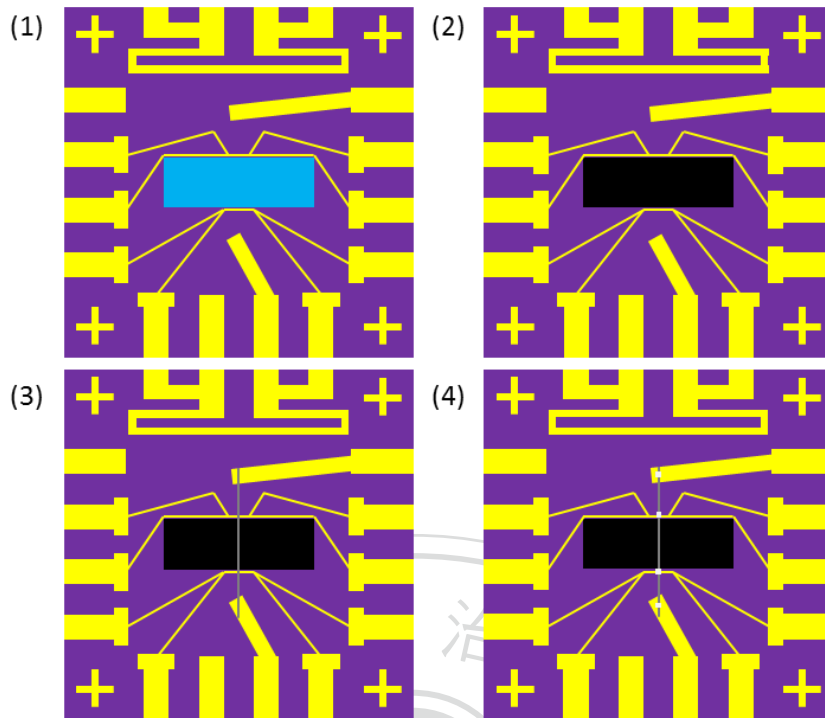
Figure 4.11 Schematic representation of suspend the nanowire and deposit the electrodes by method three. (1)Make the thermometers on the primary measurement platform by the lift-off process. (2)Break the membrane by ultrasonic wave. (3)Suspend the wire. (4)Deposit a layer of platinum to cover the contact.
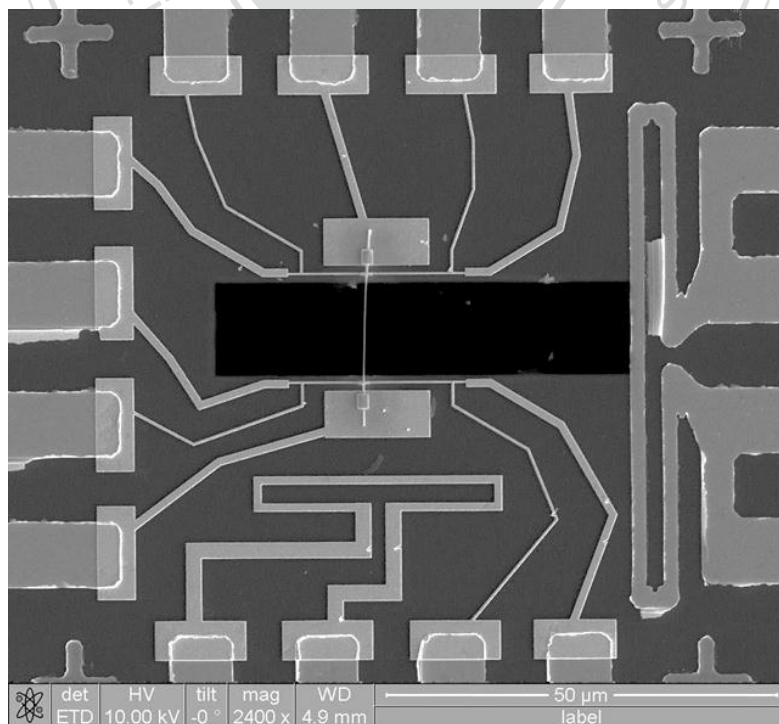
Figure 4.12 SEM image of the suspended nanowire.

4.4 Thermoelectric properties measurement of the nanowire

4.4.1 Resistivity measurement

Four-point probe method was applies to measure the resistivity. Feed an AC current via a pair of current leads into the specimen and measure the root mean square of the voltage difference via a pair of voltage leads. According to $V = IR$ and $\rho = RA/\ell$ where V, I, R, ρ, A and ℓ are voltage difference, current, resistance, resistivity, cross-section area of the wire and length between a pair of voltage leads respectively, one can get the resistivity of the nanowire.

4.4.2 Seebeck measurement

To get the Seebeck coefficient, temperature gradient is generated by heater across the sample and thermoelectric voltage that is generated by the Seebeck effect is measure. To generate the temperature gradient, the heater is placed at one end of the sample and an AC current with frequency 1ω with magnitude equals to $I \sin \omega t$ is applied to the heater. Heater would produce heat because of the Joule heating. Because heat that produced by the heater is proportional to the square of the current multiplied by the electrical resistance of the wire $Q \propto (I^2 \sin^2 \omega t)R$ where Q is the heat that produced by the heater and R is the electrical resistance of the sample and $\sin^2 \alpha = (1 - \cos 2\alpha/2)$, so the heater would be heated at frequency 2ω. As the heater is heated at frequency 2ω, the temperature fluctuation on the sample would be also at frequency 2ω. As a length of metallic wire or part of the sample is used as the sensor of the thermometer, temperature coefficient of electrical resistance of them are needed to be known at first. As temperature is fluctuated at frequency 2ω, resistance of the sensor would change at frequency 2ω. By apply a DC current to the sensor and measure the change of the voltage difference between the two end of the sensor at frequency 2ω by using lock-in amplifier, it would able to know the resistance change

of the sensor. Already knowing the temperature coefficient of electrical resistance of the sensor, how much degree different been created between two end of the sample would be known. By knowing the temperature difference and also measuring the thermoelectric voltage of two end of the sample, Seebeck coefficient can be calculated by the formula: $S = -\Delta V / \Delta T$.

4.4.3 Thermal conductivity measurement

3ω method was applied for the thermal conductivity measurement. The measurement setup is much like the setup of resistivity measurement. The specimen between the two voltage probes should be suspended to allow the temperature fluctuation. Feed an AC current of the form $I_0 \sin \omega t$ via a pair of current leads into the specimen and lock the $V_{3\omega}$ signal via a pair of voltage leads. Theoretical calculation $V_{3\omega} \approx 4I^3 LRR' / \pi^4 \kappa S \sqrt{1 + (2\omega\gamma)^2}$. By fitting the experimental data to this formula, one can get the thermal conductivity κ and thermal time constant γ of the specimen. Further detail will shoe in the

There are two ways to perform the measurement. In the first, the measurement platform is maintained at fixed temperatures, and then the frequency dependence of $V_{3\omega}$ is measured. In this way, we can check the I^3 and the $1/\sqrt{1 + (2\omega\gamma)^2}$ dependencies of $V_{3\omega}$ as well as the relation $\tan \phi = 2\omega\gamma$. In the second way of measurement, the temperature of the measurement platform is slowly increase or decrease, and the working frequency of the lock-in amplifier is changed between a few set values. The maximum working frequency is adjusted by keeping 2ωγ<4.

4.4.4 Pattern design

Several inner electrode pattern designs are use in the measurement.

Pattern one

For resistivity and thermal conductivity measure, electrodes A and B are current leads. Electrodes C and D are connected to a locking amplifier. For Seebeck measurement, part of the nanowire between the contact of electrode C and E is the high temperature sensor and part of the wire between the contact of electrode D and F is the low temperature sensor. Current via electrode A and B feed into the sensors. Electrodes C and D is a pair of voltage lead for measuring the voltage difference that is generate by the Seebeck effect.
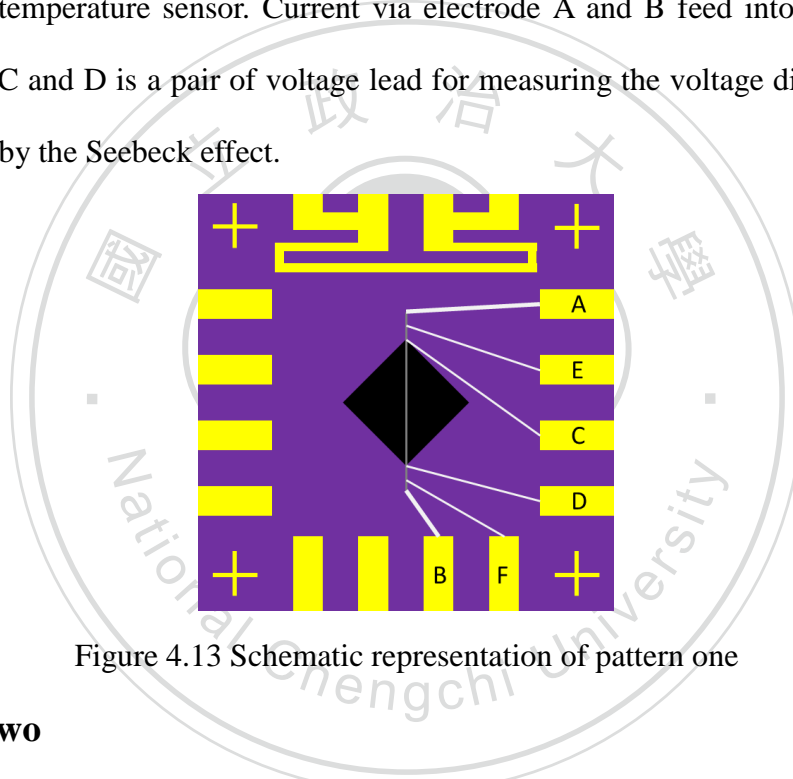

Figure 4.13 Schematic representation of pattern one

Pattern two

For resistivity and thermal conductivity measure, electrodes A and B are current leads. Electrodes C and D are connected to a locking amplifier to lock the $V_{1\omega}$ and $V_{3\omega}$ signal. For Seebeck measurement, a length of gold wire vertical to the heater between the contact of electrode G and H is the high temperature sensor of the thermometer T_h and a length of gold wire between the contact of electrode I and J is the low temperature sensor of the thermometer T_c. Current via electrode E and F feed into the thermometer T_h and T_c. Electrodes C and D is a pair of voltage lead for measuring the voltage difference that is generate by the Seebeck effect.
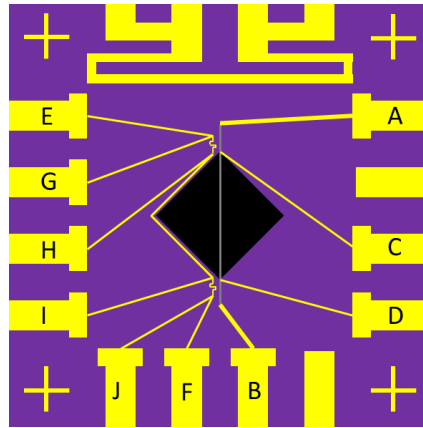
Figure 4.14 Schematic representation of pattern two

Pattern three

For resistivity and thermal conductivity measure, electrodes A and B are current leads. Electrodes C and D are connected to a locking amplifier to lock the $V_{1\omega}$ and $V_{3\omega}$ signal. For Seebeck measurement, current via electrode C and E feed into the thermometer T_h and via electrode D and F feed into the thermometer T_h. A length of gold wire parallel to the heater between the contact of electrode H and G is the high temperature sensor of the thermometer T_h and a length of gold wire between the contact of electrode I and J is the low temperature sensor of the thermometer T_c. Electrodes C and D is a pair of voltage lead for measuring the voltage difference that is generate by the Seebeck effect..
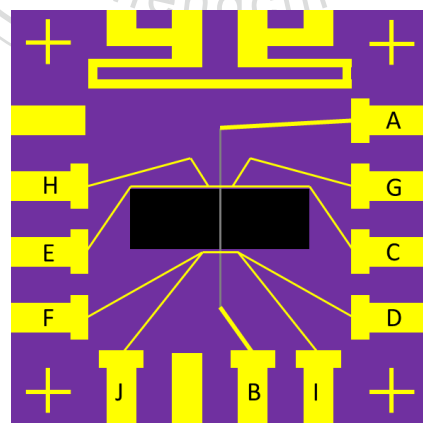

Figure 4.15 Schematic representation of pattern three

4.5 Measurement results

Resistivity measurement

The measurement of resistivity by the four-probe point method of the $Bi_{0.62}Sb_{1.38}Te_{2.74}$ nanowire with diameter 150nm was excited by a constant alternating current about 0.1μA, where it is a sine wave $I_0 \sin \omega t$ profile with constant frequency f=9.731Hz. The experimental data of resistivity in temperature range 3.5 – 300 K of the nanowire was shown in Figure 4.16. The corresponding voltage signal with less than two degree shift was picked up by the lock-in amplifier (Figure4.17).
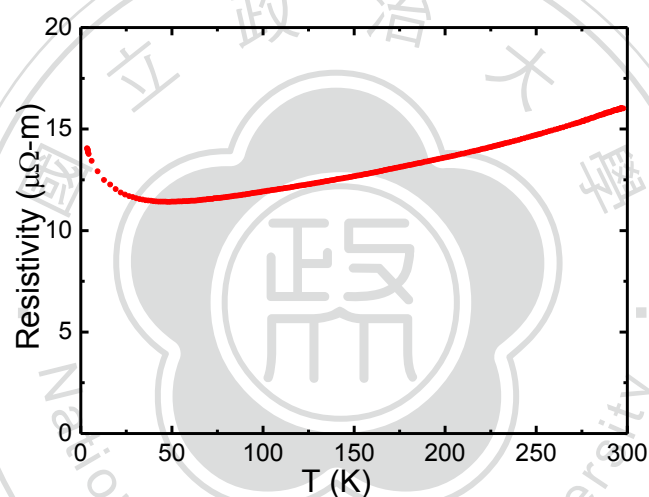

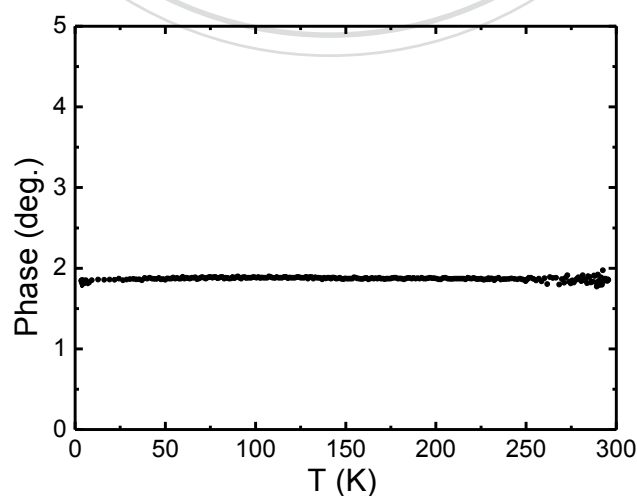Figure 4.16 The resistivity of the $Bi_{0.6}Sb_{1.4}Te_3$ nanowire with diameter 150nm.

Figure 4.17 The temperature dependence of the phase angle of V.

Seebeck measurement

Figure 4.18 shows thermoelectric voltage ΔV is linear dependence to the temperature difference ΔT at 200K. Figure 4.19 shows the obtained Seebeck coefficient from 130K to 230K.
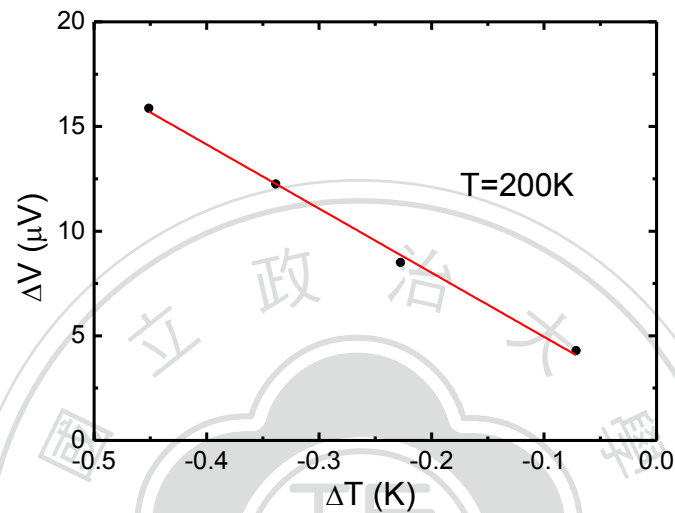

Figure 4.18 The temperature difference ΔT dependence of the thermoelectric voltage
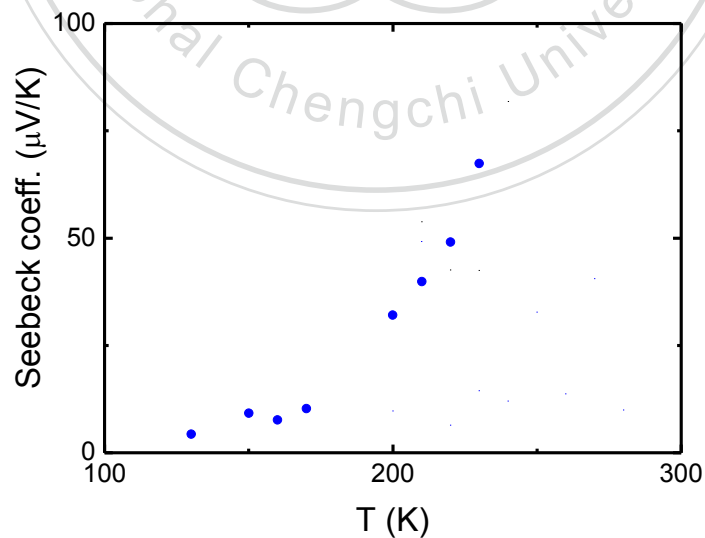
ΔV at T=200K

Figure 4.19 The Seebeck coefficient of the $Bi_{0.6}Sb_{1.4}Te_3$ nanowire with diameter

150nm.

Thermal conductivity measurement

We applied the 3ω method to measure the thermal conductivity of a suspended $Bi_{0.6}Sb_{1.4}Te_3$ nanowire with diameter 150nm by using the approximation solution: $V_{3\omega} \approx 4I^3 LRR'/\pi^4 \kappa S \sqrt{1 + (2\omega\gamma)^2}$. The calculated $R' = (dR/dT)_{T_0}$ is shown in Figure 4.20.
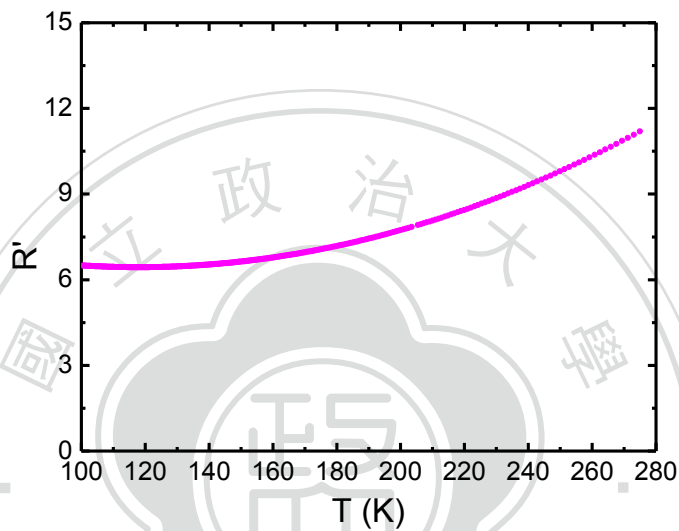

Figure 4.20 The temperature dependence of R'

There is a test for choosing appropriate exciting current. The working frequency should adjusted by keeping $\tan \phi < 4$ and experimental data of $\tan \phi$ should not curve away from linearity. The frequency dependence of the phase angle of the $V_{3\omega}$ with different exciting currents at room temperature is shown in Figure 4.21. It shows that applying 1.0μA, $\tan \phi$ linearly depend on frequency from the frequency of 5.699 to 548.525. Hence, exciting current equaled to 1.0μA was chosen for the thermal conductivity measurement. Within appropriate range of frequency and current we do find $V_{3\omega} \propto I^3$ as shown in Figure 4.22.
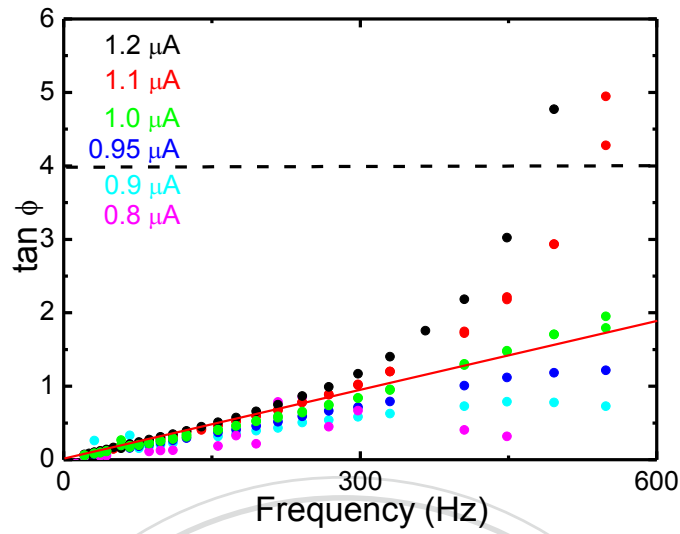
Figure 4.21 The frequency dependence of the phase angle of the $V_{3\omega}$ at room

temperature.
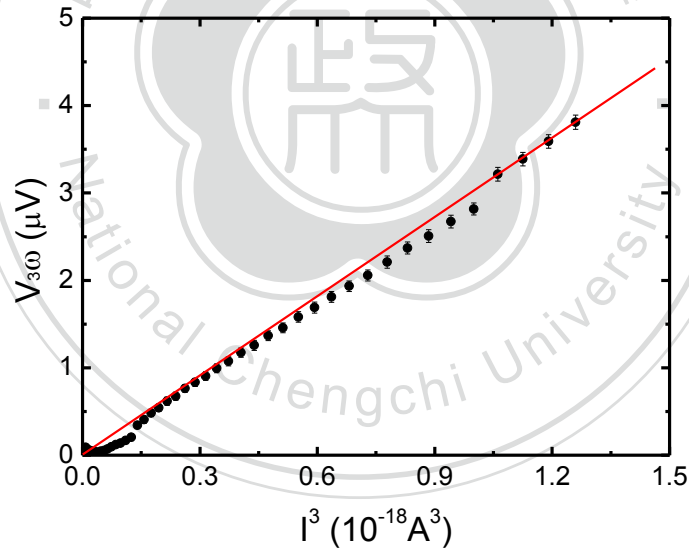
Figure 4.22 The current dependence of the $V_{3\omega}$ measured at 300K and 9.731Hz.

Figure 4.23 shows the frequency dependence of the $V_{3\omega}$ at 300K. The fitting

result from the frequency of 5.699 to 548.525 shows that $V \propto 1/\sqrt{1 + (2\omega\gamma)^2}$. The

calculated result shows that the thermal conductivity κ=3.36W/m-K at room

temperature. The thermal conductivity κ from 100K to 275K is shown in Figure 4.24.

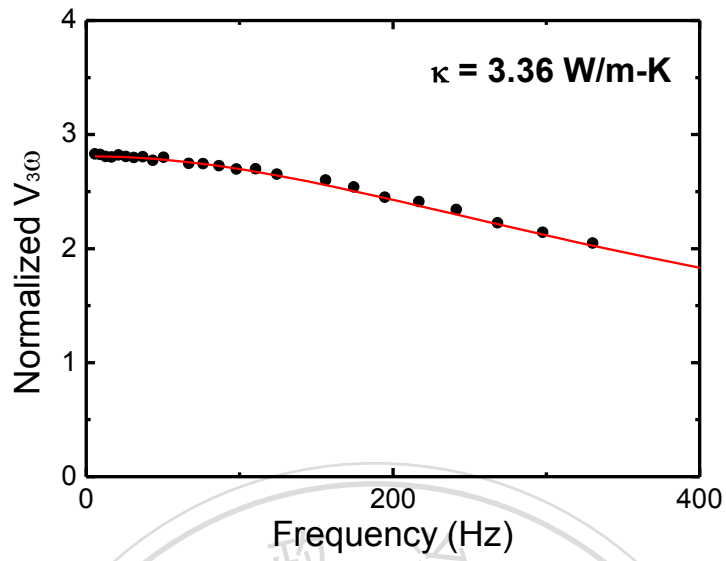Figure 4.23 The frequency dependence of the normalized $V_{3\omega}$ (solid circles) and the fitting result (solid line) at room temperature. The calculated result shows that the thermal conductivity κ=3.36W/m-K.
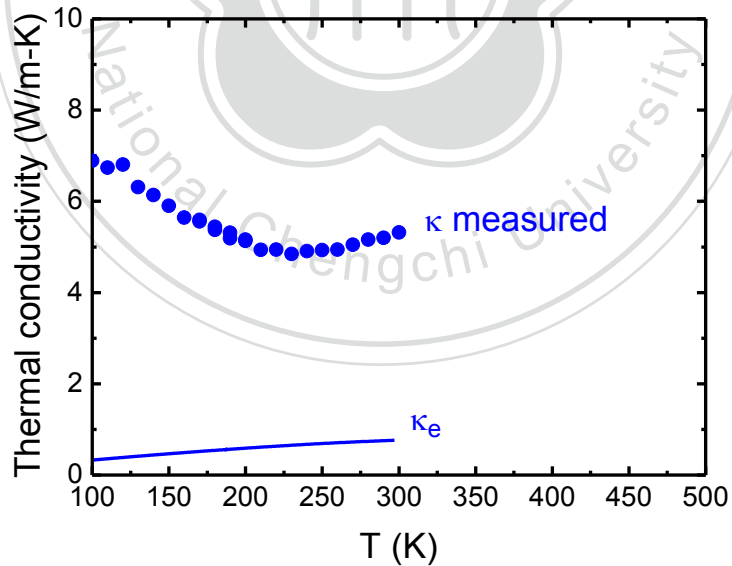

Figure 4.24 The thermal conductivity κ of the $Bi_{0.6}Sb_{1.4}Te_3$ nanowire (solid circles) and the calculated thermal conductivity by the contribution of electron (solid line).

Chapter 5

Conclusions

Single-crystalize $Bi_xSb_{2-x}Te_3$ nanowires were successfully synthesized by the stress-induced method. Nanowires grew from the $Bi_xSb_{2-x}Te_3$ films after annealing for 5~21 days at 350℃~490℃, about 60~80% of the melting temperature of the bulk materials. The diameter of the nanowires is range from few tens of nanometers to few hundreds of nanometers and the length of the nanowire is range from few micrometers to few tens of micrometers. Some wires were suspended From the TEM image, we can see that the wire is straight and uniform in diameter. STEM-EDX line-scan analysis shows that bismuth, antimony and telluride are homogenously distributed over the nanowire. STEM-EDX point-scan analysis confirmed the composition of the nanowires. According to the selected area diffraction pattern, the nanowire is single-crystalized with prefer orientation.

The technique of combining microfabrication and manipulation for suspending a single $Bi_xSb_{2-x}Te_{3-y}$ nanowire on a chip with electrodes, heater and thermometers that arrange in different patterns was developed. The resistivity ρ of the nanowire was measured by the four-point probe method. By measuring how much degree different had been created by the heater between two end of the sample and also measuring the thermoelectric voltage which was generated by Seebeck effect, Seebeck coefficient S was then calculated by the formula: $S = - \Delta V / \Delta T$. 3ω method was applied for the thermal conductivity measurement. Exciting current equaled to 1.0μA was chosen for the thermal conductivity measurement. Thermal conductivity is calculated by using the approximation solution: $V_{3\omega} \approx 4I^3 LRR' / \pi^4 \kappa S \sqrt{1 + (2\omega\gamma)^2}$. By the technique for suspending the nanowire and combine with the measurement system, one is able to measure the thermoelectric properties of the thermoelectric nanowires.

Reference

[1] L. Weber and E. Gmelin, *Transport properties of silicon*, Appl. Phys. A **53**, 136–140 (1991).

[2] Allon I. Hochbaum, Renkun Chen, Raul Diaz Delgado, Wenjie Liang, Erik C. Garnett, Mark Najarian, Arun Majumdar& Peidong Yang, *Enhanced thermoelectric performance of rough silicon nanowires*, Nature **451**, 163–167 (2008)

[3] Cheng-Lung Chen, Yang-Yuan Chen, Su-Jien Lin, James C. Ho, Ping-Chung Lee, Chii-Dong Chen and Sergey R. Harutyunyan, *Fabrication and Characterization of Electrodeposited Bismuth Telluride Films and Nanowires*, J. Phys. Chem. C **114**, 3385–3389 (2010)

[4] Jinhee Ham, Wooyoung Shim, Do Hyun Kim, Seunghyun Lee, Jongwook Roh, Sung Woo Sohn, Kyu Hwan Oh, Peter W. Voorhees and Wooyoung Lee, *Direct Growth of Compound Semiconductor Nanowires by On-Film Formation of Nanowires: Bismuth Telluride*, Nano Lett. **Vol. 9 No.8**, 2867-2872 (2009)

[5] Pollock and Daniel D., *Thermoelectricity: Theory, Thermometry, Tool*. ASTM International (1985)

[6] D.M.Rowe, Ph.D., D.Sc., *Thermoelectrics handbook,* Taylor & Francis Group, (2006)

[7] Zheng Cui, *Nanofabrication: Principles, Capabilities and Limits,* Springer (2008)

[8] L. Lu, W. Yi, and D. L. Zhang, *3 omega method for specific heat and thermal conductivity measurements*, Rev. Sci. Instrum. **Vol. 72, No. 7**, (2001)